# Long-term mineralogical and geochemical evolution of sulfide mine tailings under a shallow water cover

Michael C. Moncur[a,b], Carol J. Ptacek[a*], Matthew B. J. Lindsay[c],

David W. Blowes[a], John L. Jambor[a†]

[a]*Department of Earth and Environmental Sciences, University of Waterloo, Waterloo, ON, Canada N2L 3G1*

[b]*Alberta Innovates-Technology Futures, 360-33 Street, NW, Calgary, AB, Canada, T6N 1E4*

[c]*Department of Geological Sciences, University of Saskatchewan, Saskatoon, SK, Canada S7N 5E2*

*Corresponding author. Tel: (519) 888-4567 x 32230 Fax: (519) 746-3882

*E-mail address:* ptacek@uwaterloo.ca (C. Ptacek)

[†]Deceased

Keywords: oxidation, sulfate reduction, subaqueous, stable isotope fractionation, bacteria

## Abstract

The long-term influence of a shallow water cover limiting sulfide-mineral oxidation was examined in tailings deposited near the end of operation in 1951 of the former Sherritt-Gordon Zn-Cu mine (Sherridon, Manitoba, Canada). Surface-water, pore-water and core samples were collected in 2001 and 2009 from above and within tailings deposited into a natural lake. Mineralogical and geochemical characterization focused on two contrasting areas of this deposit: (i) sub-aerial tailings with the water table positioned at a depth of approximately 50 cm; and (ii) sub-aqueous tailings stored under a 100 cm water cover. Mineralogical analyses of the sub-aerial tailings showed a zone of extensive sulfide-mineral alteration extending 40 cm below the tailings surface. Moderate alteration was observed at depths ranging from 40–60 cm and was limited to depths > 60 cm. In contrast, sulfide-mineral alteration within the submerged tailings was confined to a < 6 cm thick zone located immediately below the water-tailings interface. This narrow zone exhibited minimal sulfide-mineral alteration relative to the sub-aerial tailings. Sulfur K-edge X-ray absorption near edge structure (XANES) spectroscopy showed results that were consistent with the mineralogical investigation. Pore-water within the upper 40 cm of the sub-aerial tailings was characterized by low pH (1.9-4.2), depleted alkalinity, and elevated $SO_4$ and metal concentrations. Most-probable number (MPN) enumerations revealed abundant populations of acidophilic sulfur-oxidizing bacteria within these tailings. Conversely, pore-water in the sub-aqueous tailings was characterized by near-neutral pH, moderate alkalinity, and relatively low concentrations of dissolved $SO_4$ and metals. These tailings exhibited signs of dissimilatory sulfate reduction (DSR) including elevated populations of sulfate reducing bacteria (SRB), elevated pore-water $H_2S$ concentrations, and strong $\delta^{34}S$-$SO_4$ and $\delta^{13}C$-DIC fractionation. Additionally, mineralogical investigation revealed the presence of secondary coatings on primary sulfide minerals, which may serve as a control on metal mobility within the sub-aqueous tailings.

Results from this study provide critical long-term information on the viability of sub-aqueous tailings disposal as a long-term approach for managing sulfide-mineral oxidation.

## 1. Introduction

Extraction and processing of base and precious metals from sulfide-ore deposits generates large volumes of sulfide tailings. When tailings are exposed to oxygen, sulfide minerals within the tailings will oxidize generating acidity, releasing elevated concentrations of dissolved $SO_4$, metals and metalloids to the pore water (Nordstrom and Alpers, 1999; Blowes et al., 2013). The rate of sulfide oxidation is greatest immediately after mine tailings are deposited because at this time, sulfide minerals surfaces are fresh and the $O_2$-diffusion path is shortest (Gunsinger et al., 2006). Therefore, following deposition, it may be desirable to control atmospheric $O_2$ entry into the tailings through the addition of a barrier or cover over the mine wastes. Physical barriers that have been applied or proposed include dry covers composed of fine-grained materials to maintain high water contents (Rasmusson and Collin, 1987; Nicholson et al., 1989; Yanful et al., 1994; Ouangrawa et al., 2009; Dobchuk et al., 2013; Lu, et al., 2013); covers composed of geosynthetic materials (Sodermark and Lundgren, 1988; Lewis and Gallinger, 1999; Rowe and Hosney, 2013); and covers containing $O_2$-consuming materials (Reardon and Moddle, 1985; Broman et al., 1991; Tassé et al., 1994); In addition to limiting $O_2$ diffusion, covers also contain the tailings and protecting them from wind and water erosion (Kossoff et al., 2014).

Water covers offer an alternative approach to dry covers for managing sulfide-mineral oxidation. Sub-aqueous tailings deposition has potential to limit sulfide-mineral oxidation and associated environmental impacts (e.g., Hamilton and Fraser, 1978; Pedersen et al., 1993; Yanful and Simms, 1997; Jacob and Otte, 2004; Vigneault, 2007). The $O_2$ ingress into tailings is limited by the low diffusion coefficient of the water cover. For example, the diffusive flux of $O_2$ to water

covered tailings may decrease by up to 10,000 times relative to sub-aerial tailings (Robertson et al., 1997; Awoh et al., 2013). Suppression of sulfide-mineral oxidation therefore may be accomplished by disposal of tailings into lakes or deep marine environments (Pedersen et al., 1985; Pedersen et al., 1993; Poling et al., 2002), or by the construction of wet covers on existing tailings impoundments (Robertson, 1992). A number of laboratory and field studies have investigated the short-term storage of tailings under shallow water covers (Davé et al., 1997; Li et al., 1997; Holmström and Öhlander, 1999; Vigneault et al., 2001; Elberling and Damgaard, 2001; Samad and Yanful, 2005), but only a few studies have considered the reactivity of tailings that have been submerged over long time periods (e.g., Jacob and Otte, 2004, Vigneault et al., 2007).

The objective of this study was to understand the biogeochemical processes that have occurred within sulfide mine tailings subjected to over 60 years of storage under a 100 cm water cover. This study involved detailed analyses of mineralogy of powder and thin section samples, geochemical analyses of tailings pore-water and solids, stable isotope analyses of pore water, and enumerations to identify active microbial populations within the tailings.

## 2. Study Site

The former Sherritt-Gordon Zn-Cu Mine is located in Sherridon, approximately 800 km northwest of Winnipeg, MB, Canada (Fig. 1). The site is situated near the southern edge of the Precambrian Shield in a region characterized by long, cold winters and cool summers. Monthly average temperatures range from –21°C in January to 18°C in July and the mean annual temperature is 0.5°C (Environment Canada, 2012). The long-term average precipitation for Flin Flon, which is 60 km SW of the site, is 463 mm year^{-1}, which is fairly similar to the total

precipitation in Sherridon (Moncur et al., 2014). Evapotranspiration losses in the Sherridon area are approximately 350 mm annually (Hydrological Atlas of Canada, 1978).



Fig. 1. Location of the former Sherritt-Gordon Zn-Cu mine in Sherridon, Manitoba, Canada.

Two Precambrian Zn-Cu volcanogenic massive sulfide ore bodies were exploited to produce Zn and Cu concentrates with minor amounts of Au and Ag. Each ore body was approximately 5 m thick and occurred as lenticular layers of massive and disseminated sulfides, and as irregular remobilized masses (Goetz and Froese, 1982). The ore averaged 2.5 wt. % Cu, 3.0 wt. % Zn, 0.62 g/t Au and 20 g/t Ag (Farley, 1949). Ore-zone sulfides were, in decreasing order of abundance, pyrite [$FeS_2$] and pyrrhotite [$Fe_{(1-x)}S$] (2:1 ratio), chalcopyrite [$CuFeS_2$], sphalerite [$ZnS$], and accessory cubanite [$CuFe_2S_3$]. Farley (1949) reported trace arsenopyrite [$FeAsS$] occurring as small grains within pyrrhotite, native gold, and irregular occurrences of galena [$PbS$] in veinlets and disseminations within hanging-wall shear zones in the gneiss host rock. From 1931 to 1951, a total of 7.7 Mt of pyritic ore was milled to produce 0.17 Mt of Cu, 0.14 Mt of 50 percent Zn concentrate, and minor amounts of Ag (91000 kg) and Au (2900 kg) (Mineral Resources Branch, 1978).

Sulfide tailings from the mining operations were discharged into three separate tailings impoundments containing a combined 7.4 Mt and occupying an area of 47 ha. The Camp Tailings were deposited between 1931 and 1932 and the Woods Tailings were deposited between

1937 and 1951. Tailings were deposited into Fox Lake at the end of mining in 1951. Extensive sulfide-mineral oxidation within the Camp and Woods tailings has generated pore-waters with low pH values and extremely elevated concentrations of dissolved sulfate and metals (Moncur et al., 2005; Moncur et al., 2009a). Discharge of surface water and groundwater from the tailings deposits into adjacent Camp Lake has severely degraded water quality (Moncur et al., 2006). Effluent from Camp Lake flows into Kissising Lake where concentrations of Zn and Cu in the bottom sediments were elevated well above background concentrations in an area covering 9.5 $km^2$ (Moncur et al., 2014).

Fox Lake is a small (700 m by 300 m) lake situated in a semi-closed basin with one outflow. The lake overlies Precambrian Shield rock of the Sherridon Group, consisting of both metasedimentary and metavolcanic rocks (Goetz and Froese, 1981). The Fox tailings were slurried and discharged into Fox Lake from a number of spigot lines. This deposit extends from the shoreline outward into Fox Lake where the majority of tailings were submerged as several lobes that form small exposed islands (Fig. 2). The exposed tailings were visually oxidized and did not support vegetation. In contrast, much of the submerged tailings were overlain by a layer of naturally established vegetation and detritus.

Fig. 2. Aerial photos of Fox Lake and the submerged tailings between 1952 and 2007. Images taken a) 1952; b) 1968; c) 1977; d) 1983; e) 2001; f) 2007. Image (e) shows where samples were collected form the tailings on-land (FX) and submerged under a 100 cm water cover (FXS). Image from 2007 courtesy of Google Earth.

## 3. Methods

### 3.1. Core collection and piezometer installation

Air photos and satellite images were used to identify areas within the Fox tailings where samples representative of sub-aqueous and sub-aerial tailings could be collected. Core samples were collected in August 2001 and August 2009, at two locations from the Fox tailings; an exposed sub-aerial tailings location (FX), and a sub-aqueous tailings location characterized by an approximately 100 cm water cover (FXS) (Fig. 2). Two cores extending from the tailings surface to a depth of 100 cm were collected from each location. One core was used to obtain pore-water samples and the other to obtain samples of tailings solids. Core samples were cut into 25 cm sections, capped and sealed, and immediately stored in a freezer at -20˚C until analysis. Additional core samples were collected in August 2006 at each location and stored at 4˚C for

microbial enumerations. Drive-point piezometers measuring 1.3 cm in diameter and screened over the bottom 5 cm were installed into the submerged tailings in August, 2009, to depths of 12, 38, 63 and 88 cm below the water-tailings interface. These piezometers facilitated collection of larger pore-water volumes than could be obtained by squeezing pore-water from 2001 core samples. *3.2. Solid phase analyses and mineralogy*

Core collected for solid analyses was split by sawing cores while frozen, and one half was analyzed for total metals, sulfur, carbon and grain-size distribution, and the other half for mineralogy. Discrete samples were collected along the length of core where visual changes were observed. Samples of tailings solids from FX and FXS were analyzed for total metal concentrations using a HF/HNO$_3$ extraction followed by inductively coupled plasma – optical emission spectrometry (ICP–OES) detection. Total extractable carbonate was measured using the method of Barker and Chatten (1982), and total sulfur (S) and carbon (C) were determined by combustion and infrared detection using a C and S analyzer (LECO Corporation, USA). Physical properties of the FX and FXS tailings collected in 2001 were determined through grain-size analysis using standard sieves sizes. The porosity (n) of the tailings was calculated using the method of Istomina (1957), where $n = 0.225(1 + 0.83^{C_U})$. The uniformity coefficient is represented by $C_U$, where $C_U = D60/D10$.

Primary crystalline phases in the tailings, collected in 2001, were identified through X-ray diffractometry (XRD) using a Siemens rotating-anode instrument. Polished thin sections of the core samples were prepared without the use of water, thereby minimizing the dissolution of readily soluble minerals. These sections were examined by optical microscopy, using both transmitted and reflected light. Areas of interest were marked on the section and photos were taken to assist in location of the relevant grains during examination by scanning electron

microscopy–energy dispersive spectrometry (SEM-EDS). The SEM-EDS utilized a Phillips XL-30 instrument with a coupled energy-dipersion analyzer. Using a fully-automated Cameca SX50 scanning electron-microprobe, thin sections were analyses to provide an indication of compositional variation of select minerals.

Bulk S K-edge X-ray absorption near edge structure (XANES) spectra were collected from tailings on the SXRMB beamline (06B1-1) at the Canadian Light Source (Saskatoon, SK, Canada) to identify oxidized and reduced sulfur species. Frozen core samples obtained in 2009 were freeze-dried under vacuum at -45°C and pulverized in an agate mill. The powdered samples were then mounted with carbon tape on a copper plate and transferred into the vacuum chamber on the SXRMB end station. The monochromator used a Si (111) crystal and replicate spectra were collected in total electron yield (TEY) mode for samples ($n = 3$) and reference materials ($n = 2$) including pyrite, pyrrhotite, chalcopyrite, sphalerite, galena, chalcopyrite, elemental sulfur [$S_8$], gypsum [$CaSO_4 \cdot 2H_2O$], and jarosite [$KFe_3(OH)_6(SO_4)_2$]. Additional spectra for chalcocite [$Cu_2S$] and covellite [$CuS$] were obtained from SXRMB beamline scientists. Data processing and analysis was performed using ATHENA, which is part of the IFEFFIT software suite (Ravel and Newville, 2005). All spectra were calibrated to the theoretical $S_8$ K-edge energy ($E_0$; 2472.0 eV) according to first derivative maxima. Linear combination fitting (LCF) of normalized spectra was constrained by fixing $E_0$ values to calibrated energies and limiting total reference spectra to four, except when additional phases were identified by XRD and/or petrographic examination.

### 3.3. Aqueous geochemistry

The squeezing method described by Moncur et al. (2013) was used to extract pore-water from cores collected in 2001 and 2009 from FX and in 2001 from FXS. From each location a

continuous 100 cm core was collected for squeezing and cut into 25 cm sections. Each core-section top was fitted with a sealed plunger and the bottom was fitted with a sealed base with an outlet port to collect expelled water. Pressure was applied to the plunger to displace the pore-water downward through the core. Resulting water was collected into 60 mL polyethylene (PE) syringes, filtered through 0.45 µm surfactant free cellulose acetate membranes, and transferred to prewashed PE bottles. One aliquot was acidified with 12 N trace-metal grade $HNO_3$ to a pH of less than 2 for cation analysis, and other aliquots were left unacidified for analyses of inorganic anions and stable isotope ratios of $\delta^{34}S$, $\delta^{18}O_{SO4}$, $\delta^{18}O$ and $\delta^2H$.

Determinations of pore-water Eh and pH were made at least three times during squeezing to ensure results were representative. The Eh was measured using a platinum combination redox electrode (96-78BN; Thermo Scientific, USA), which was checked against ZoBell's (Nordstrom, 1977) and Light's solution (Light, 1972). The pH was measured using a Ross combination electrode (815600; Thermo Scientific, USA) calibrated with standard buffer solutions at pH 7, 4, and 1. Measurements of alkalinity were made on filtered samples by titrating with 0.16N $H_2SO_4$ to the bromcresol green–methyl red endpoint (pH 4.5).

Pore water from piezometers installed in the submerged tailings was collected with a peristaltic pump using 0.64 cm diameter PE tubing. The piezometers were pumped dry and allowed to recover prior to sampling. Measurements of Eh and pH were made in the field using a sealed flow-through cell that was maintained near groundwater temperature. The pH electrode was calibrated and the performance of the Eh electrode was checked before each measurement. The temperature was measured from each piezometer in situ using a down-hole temperature probe. Water samples were collected following methods as described above with additional samples collected for the analyses of dissolved organic carbon (DOC) and hydrogen sulfide

(H$_2$S). To prevent atmospheric contamination, samples for $\delta^{13}C_{DIC}$ and $\delta^{18}O_{CO3}$ determination were collected by filling a 60 mL syringe with water directly from the peristaltic pump tubing. Water from the syringe was then injected into 100 mL vacuum-sealed glass bottles fitted with Teflon-lined septa. Surface water samples were collected near the shore of Fox Lake using a 60 mL PE syringe held approximately 5 cm below the lake surface annually between 2001 and 2009 following the same procedures as above.

All water samples were immediately refrigerated at 4°C until analysis. Water samples were analyzed using ICP-OES for major cations, inductively coupled plasma-mass spectrometry (ICP-MS) for trace elements, and ion chromatography (IC) for anions. Combustion and infrared detection were used for DOC analysis. Dissolved H$_2$S was determined using the methylene blue procedure (SMEWW, 2005). Sulfur-isotope ratios of dissolved sulfate were determined by adding BaCl$_2$ to precipitate BaSO$_4$, which was then converted into SO$_2$ in an elemental analyzer coupled to a mass spectrometer in continuous flow mode (Giesemann et al., 1994). Sulfur-isotope measurements are reported in delta notation ($\delta^{34}S$) relative to the Vienna Canyon Diablo Troilite (V-CDT) standard. Oxygen-isotope analysis on BaSO$_4$ samples was carried out by pyrolysis in a high temperature conversion/elemental analyzer - interfaced to an isotope-ratio mass spectrometer. Values of $\delta^{34}S$ and $\delta^{18}O$ in sulfate were measured to identify reactions affecting sulfate concentrations including oxidation of pyrite and bacterially mediated sulfate reduction. The oxygen isotopic composition of water samples was determined by the H$_2$O–CO$_2$ equilibration method (Nelson, 2000). Hydrogen (deuterium) isotopic composition in water was measured on an isotope ratio mass spectrometer determined by reduction of water to H$_2$ gas using chromium metal as an active reducing agent. The results of oxygen and deuterium isotope measurements are expressed in delta notation ($\delta^{18}O$ and $\delta^2H$) relative to Vienna Standard Mean

Ocean Water (V-SMOW) standard. The $\delta^{18}O$ and $\delta^2H$ composition of surface and pore water was measured to identify the degree of evaporative enrichment and groundwater surface water interactions. The method of Assayan et al. (2006) was used to determine $\delta^{13}C$ on dissolved inorganic carbon, reported relative to Vienna Pee Dee Belemnite (V-PDB) standard. The $\delta^{13}C$ of dissolved inorganic carbon (DIC) was used to identify processes such as carbonate dissolution and bacterial sulfate reduction.

### 3.4. Microbial enumerations

To identify bacterial populations that could be catalyzing oxidation and reduction reactions in the tailings, enumerations of neutrophilic sulfur-oxidizing bacteria (nSOB), acidophilic sulfur-oxidizing bacteria (aSOB), acid-producing (fermentative) bacteria (APB), sulfate-reducing bacteria (SRB), and iron-reducing bacteria (IRB) were performed using a five-tube most probable number (MPN) approach (Cochran, 1950). Methods for preparation, inoculation, and enumeration of nSOB and aSOB are described in detail by Blowes et al. (1996). Briefly, the nSOB and aSOB media containing $Na_2S_2O_3 \cdot 5H_2O$ as the electron donor and the final pH was adjusted to 7.0 and 4.2, respectively. Media were filter sterilized and 9 mL aliquots were dispensed into sterile culture tubes. As described by Lindsay et al. (2011), APB were grown in a saccharide and peptide medium (Hulshof et al., 2003), whereas IRB and SRB were grown in Fe(III) EDTA (Gould et al., 2003) and modified Postgate C (Blowes et al., 1996) media, respectively. Culture tubes were filled with 9 mL aliquots of the APB medium, capped, and sterilized. Media for IRB and SRB enumerations were dispensed in 9 mL aliquots into 20 mL serum vials, which were then crimp-sealed and sterilized. All growth media were inoculated with 1.0 g of sample from refrigerated core samples within 30 days of collection. Sample handling and inoculation for the SRB and IRB enumerations were performed in an anaerobic chamber.

Enumeration of positive results was performed after 48 hours for APB and after four weeks for nSOB, aSOB, IRB, and SRB.

### 3.5. Geochemical modeling

Pore-water chemistry data were interpreted with the assistance of the equilibrium chemical-speciation/mass-transfer model MINTEQA2 (Allison et al., 1990). The MINTEQA2 database was modified for consistency with the WATEQ4F database (Ball and Nordstrom, 1991). Additional solubility data were incorporated for siderite (Ptacek and Blowes, 1994) and Co (Papelis et al., 1991). Saturation indices were calculated for discrete minerals that may control concentrations of dissolved ions in pore-waters.

## 4. Results and Discussion

### 4.1. Fox Lake water level

Information on methods of tailings deposition into Fox Lake is limited. Water levels in Fox Lake were not recorded during or after tailings deposition; therefore, it remains unclear if there were periods during the past 60 years when the tailings may have been exposed to oxygen. In the absence of water level data, air photos of the Fox Tailings taken between 1952 and 2008 were used to gain some information about the history of the tailings (Fig. 2). Due to the poor resolution and high reflectance of the 1952 image, it is difficult to determine the extent of water cover over the tailings; however, subsequent images of the tailings from 1968 to 2008 show that the majority of the tailings remained submerged. Minimal water level fluctuations of Fox Lake were observed during annual visits between 2000 and 2009. The water table elevation in the land-based tailings was 50 cm below the ground surface in 2001 and 2009. Hydraulic head data from piezometers installed in the submerged tailings at FXS combined with water level data from Fox Lake showed the absence of a vertical hydraulic gradient, suggesting that there was no

advective flow between the water cover and underlying pore water. . The hydraulic gradient

between FX and FXS was not determined.

## 4.2. Physical tailings characteristics

Grain-size distributions were measured on samples extracted at various depths from the FX and

FXS tailings showing a well sorted, fine to medium grain sand (Fig. 3). Average calculated $C_U$

values from the FX and FXS tailings was similar at 2.6 and 2.9, respectively, representative of a

uniform grain-size distribution (Fig. 3). A perfectly uniform sediment such as dune sand has a

$C_U = 1$, whereas a poorly sorted glacial till has a $C_U = 30$. The uniform sorting and relatively low

silt content in both tailing profiles suggests deposition was near the spigot point (Robertson,

1994). The $D_{10}$ (mm) of the tailings, which is the grain-size diameter at which 10% by weight of

the particles are finer, showed that values from both profiles were almost identical below a 40

cm depth, however, the grain size was much coarser in the FX tailings above 40 cm. The coarser

nature of the FX tailing above 40 cm is not due to a physically larger grain-size, but a result of

sulfide oxidation followed by Fe (oxy)hydroxide precipitation causing formation of cemented

grain-clusters and coatings to form on primary mineral surfaces. The calculated porosities of

both tailings profiles were similar, ranging from 0.40 and 0.42, typical of sand (Freeze and

Cherry, 1979). Grain size distributions measured from the FXS tailings and the FX tailings

below a 40 cm depth and were similar to those measured in the unoxidized Camp Tailings
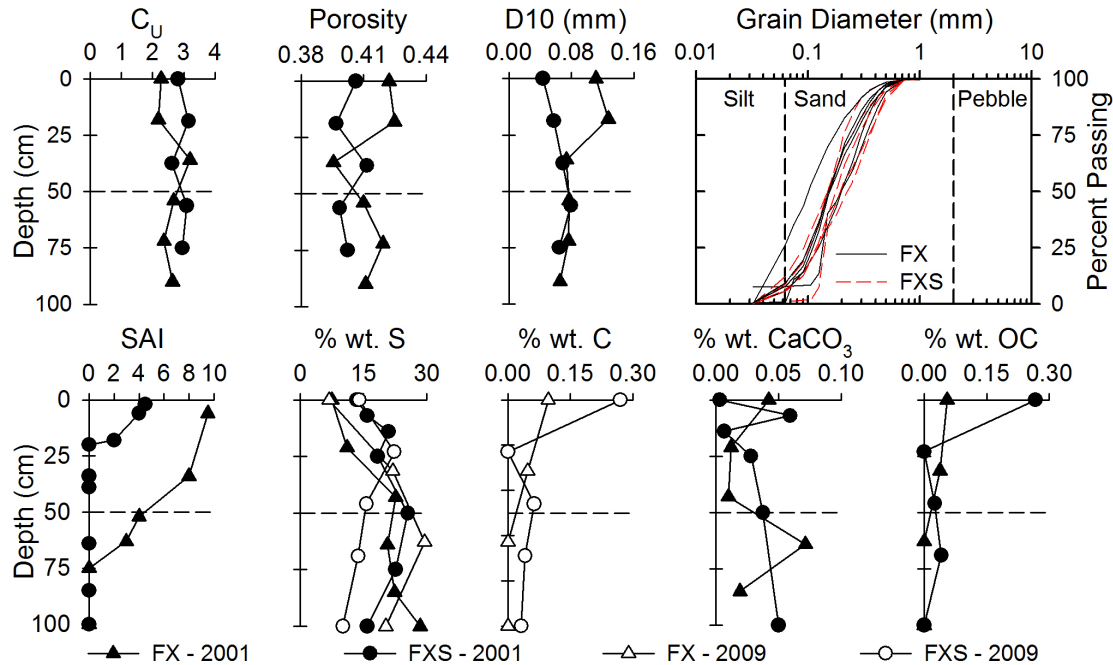
(Moncur et al., 2005).

Fig. 3. Depth profile through the on land (FX) and submerged tailings (FXS), top row showing the uniformity coefficient ($C_U$), porosity, and grain–size distribution. The bottom row shows the sulfide alteration index (SAI) and weight percent of total sulfur (S), carbon (C), carbonate minerals ($CaCO_3$), and calculated organic carbon (OC). The water-tailings interface is located at a depth of 0 cm for FXS and the dashed line represents the water table at FX.

### 4.3. Mineralogy

Optical microscopy and XRD analysis of the non-opaque assemblage in the unaltered tailings indicate the presence of quartz, albite, and microcline, with smaller amounts of amphibole, muscovite and biotite. Accessory amounts of sillimanite and chlorite were detected. Carbonate minerals were not observed during this study; however, Moncur et al. (2005) reported trace amounts of primary siderite in the Camp Tailings. Sulfide minerals comprised up to 28 wt. % of the unaltered Fox Tailings. The principal sulfides were pyrite and pyrrhotite with minor amounts of sphalerite and trace chalcopyrite also observed. Secondary Fe (oxy)hydroxides were abundant in the ochreous zone of both the on-land and submerged tailings, with goethite being the only Fe oxyhydroxide detected in the X-ray diffractograms in all samples examined.

### 4.3.1. Sub-aerial tailings

Extensive sulfide oxidation of the sub-aerial tailings was observed in the tailings likely exposed for six decades to atmospheric oxidation. The tailings were characterized by an ochreous zone of extensive oxidation that extended from the surface to a depth of 40 cm. This zone was underlain by a transitional zone of weaker oxidation and unaltered tailings beginning at a 60 cm depth. Optical microscopy was used to assess the sulfide alteration intensity (SAI), which is classified on a scale of 1 to 10 developed by Blowes and Jambor (1990) and refined by Moncur et al. (2005; 2009). For example, at a SAI = 10, the sulfides have been almost completely obliterated; at SAI = 3, remnant cores of pyrrhotite are abundant; and at SAI = 1, the alteration occurs only as narrow rims on pyrrhotite. The SAI was determined on tailings samples collected from FX and FXS in 2001 (Fig. 3).

Samples from the uppermost 6 cm of the ochreous zone contained numerous grains of pyrite and chalcopyrite, but pyrrhotite and sphalerite were not observed (Fig. 4A). The proportion of chalcopyrite to pyrite was higher than observed in the unaltered tailings with some of the chalcopyrite grains showing irregular margins possibly due to leaching. Pyrite lacked alteration rims but many of the grains had smooth margins bounding a shard-like habit that was not observed in unaltered tailings. Furthermore, pyrite was noticeably sparse relative to its abundance in the deeper unaltered tailings and Fe (oxy)hydroxides were abundant. A majority of sulfide minerals had been consumed by oxidation; therefore, an SAI of 9 was assigned to these samples (Fig. 3). Unlike the older Camp Tailings where extensive near-surface sulfide oxidation had resulted in almost complete destruction of soluble Al-silicate minerals (e.g., biotite, chlorite) and extensive alteration to albite and amphibole (Moncur et al., 2005), Al-silicate alteration in these sub-aerial tailings was limited to minor biotite replacement by Fe (oxy)hydroxides and

minimal replacement of muscovite by Fe-oxyhydroxide along the basal cleavage planes. Other than the presence of Fe (oxy)hydroxides, which are associated with all minerals, no other evidence of secondary replacement of Al-silicate minerals was observed.

The pyrite content was greater at depth of 33-35 cm, but remained approximately 25 % of that typical of unaltered samples. The SAI from 33-35 cm was 8 (Fig. 3). A few grains of chalcopyrite were present, but pyrrhotite and sphalerite were not observed. Similar to the upper 6 cm zone, samples at a 33-35 cm depth were strongly ochreous, however at both depths, Fe (oxy)hydroxides did not cement the particles into large aggregates, and in both zones, the greatest concentration of the Fe (oxy)hydroxide was associated with the smaller particles.

The oxidation intensity declined at a depth of 51-54 cm, which corresponded to the water table depth. Abundances of pyrite and pyrrhotite at this depth were typical of those found in unaltered tailings. Several grains of sphalerite were also observed, marking the first appearance of this sulfide within the tailings profile. Although pyrrhotite alteration was observed throughout the profile, the variation of alteration was predominantly from narrow to thick rims of marcasite, surrounding residual cores of unaltered pyrrhotite. Complete pseudomorphs after pyrrhotite were present, but they were much less common than particles containing residual pyrrhotite. The SAI at this depth is assigned to be 4 (Fig. 3). Polished thin sections did not exhibit megascopic ochreous particles, but particles observed microscopically with transmitted light had exteriors stained by Fe (oxy)hydroxides that were too sparse to appear as discrete rims in reflected light.

Samples observed at depths of 62-65 and 72-75 cm were similar in that both contained abundant pyrite and pyrrhotite, with accessory amounts of sphalerite > chalcopyrite. At a depth of 62-65 cm, some pyrrhotite grains exhibited alteration rims of marcasite and a SAI of 4 was

assigned (Fig. 4C). The pyrrhotite was fresh at a depth below 72 cm and the SAI assigned was 0
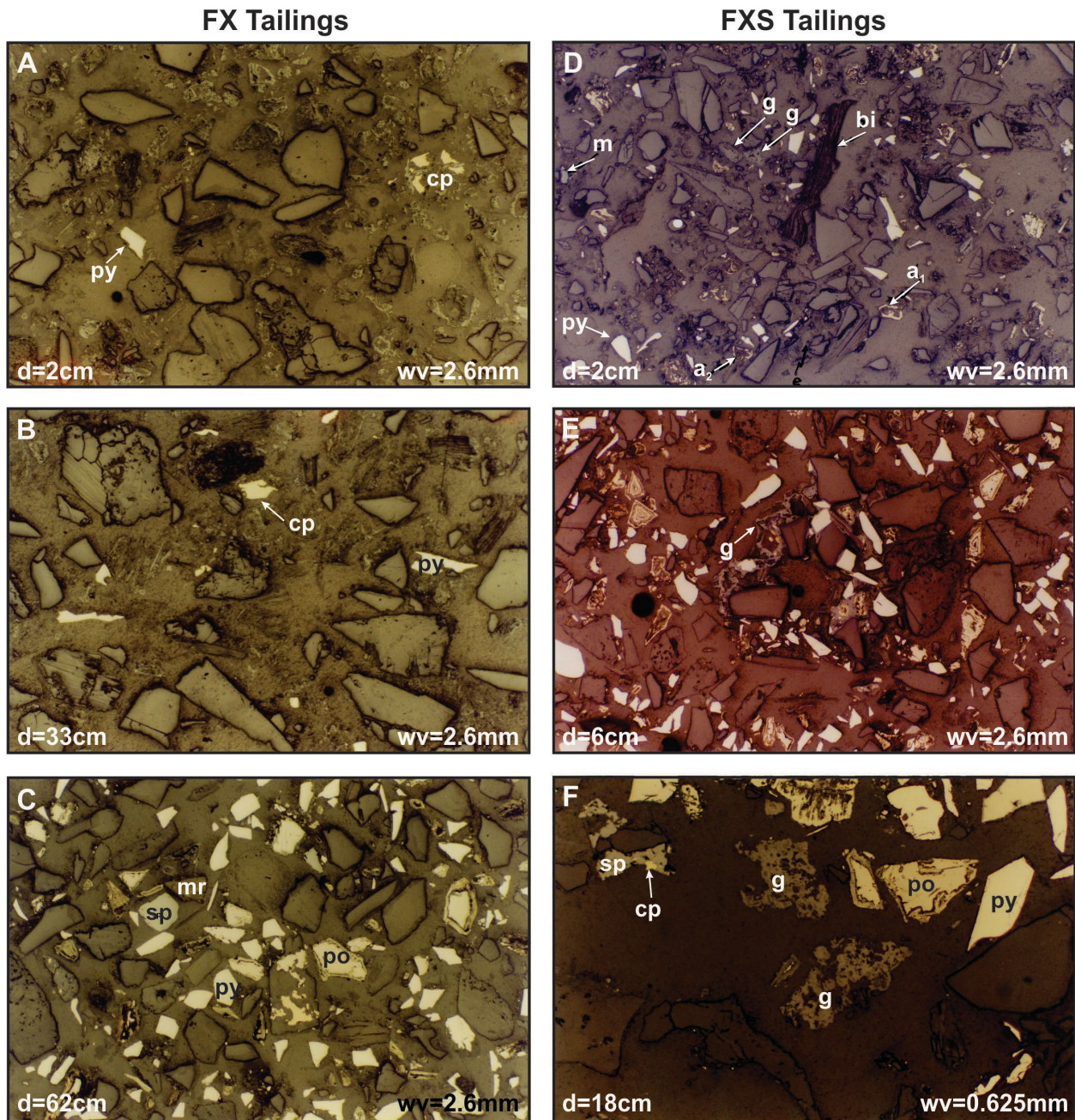
(Fig. 3).



Fig. 4. Photomicrographs of tailings thin sections in plane-polarized reflected light (A) 2 cm depth in the sub-aerial tailings (FX) showing a single grains of whitish pyrite (py) and yellow chalcopyrite (cp) which are the only remaining sulfides (B) FX 33 cm depth showing sparse pyrite and chalcopyrite (C) FX 62 cm depth showing unaltered pyrite; the grey grain is sphalerite (sp). Pyrrhotite (po) is variably rimmed by marcasite (mr) and in some grains complete replacement by marcasite.; (D) 2 cm depth in the sub-aqueous tailings (FXS) showing unaltered

pyrite with pyrrhotite extensively replaced mainly to complete pseudomorphism by marcasite. Grey magnetite (m), brown biotite (bi) lath and two irregular patches of grey goethite (g) are detectable. (E) FXS at a 6 cm depth showing abundant pyrite, altered pyrrhotite, and a grey Fe oxyhydroxide cement surrounding various gangue minerals. (F) FXS 18 cm depth showing unaltered pyrite, a sphalerite grain with a chalcopyrite inclusion, and cores of pyrrhotite with a thin exterior of marcasite. Two irregular patches of grey goethite are present. Depth and width of view are represented by d and wv, respectively.

### 4.3.2. Sub-aqueous tailings

In contrast to the observed oxidation zone in the sub-aerial tailings, the equivalent ochreous zone in the submerged tailings extended only 6 cm below the water-tailings interface. The SAI value assigned to these shallow tailings is 4.5 (Fig. 3). Petrographic examination of tailings collected from a depth of 2 cm revealed major amounts of pyrite with no visible alteration. At this depth, pyrrhotite exhibited similar to greater abundance than pyrite, and occurred sparingly as residual cores. More than 95 percent of the pyrrhotite at this depth had been pseudomorphically replaced as a rim of marcasite surrounding a hollow core (Fig. 4D). Unaltered chalcopyrite was present in trace quantities and sphalerite was absent with the exception of a single grain that occurred as an intergrowth with chalcopyrite.

Goethite was common as irregular patches, but rims on individual particles were poorly developed and incomplete. Cementation of groups of particles by goethite occurred only locally where clots and patches of goethite form a matrix rather than inter-particle binding agent. Over 20 particles in the polished thin section were examined by SEM-EDS analyses to determine the compositions and their variations among different areas and textures of Fe oxyhydroxide. All spectra were similar with small amounts of S, Al, and Si consistently present. Several of the centers within the marcasite pseudomorphs were also examined using SEM-EDS. All except one of the centers were devoid of minerals. The ratio of the peak heights for Fe and S resembled those of pyrrhotite (i.e., Fe:S = ~1:1); however, the reflectance of the mineral was characteristic

of a sulfate rather than sulfide phase. Therefore, the former mineral in the dark centers of the pseudomorphs was presumably melanterite, which was abundant in the X-ray diffractogram of the underlying sample from 6 cm. The rapid dissolution of melanterite in water (Chou, et al., 2013) would explain its absence.

Mica observed was predominantly muscovite, but biotite was formerly the more abundant of the two prior to its extensive replacement by Fe (oxy)hydroxides and lesser amounts of hydrobiotite. Replacement of muscovite has been minimal and was restricted to Fe-oxyhydroxide occurrences along the basal cleavage, as observed in the on land-tailings.

The ochreous zone at the top of the FXS core was less than 6 cm thick and was megascopically distinctive due to the orange color. Samples collected at a 6 cm depth consisted of blackish tailings that were directly below the ochreous zone. Optical microscopic examination revealed that the principal non-opaque gangue assemblage at 6 cm was similar to that in the overlying ochreous tailings, and a bulk XRD confirmed that the similarity extended to the presence of detectable hydrobiotite and a small amount of kaolinite (~2%). One of the main differences between 6 cm depth and the overlying ochreous tailings is that goethite was less abundant and did not occur as coatings on primary sulfides. Petrographic examination revealed that goethite occurred only in small areas as an intergranular fill and as rims observed on the adjoining gangue minerals (Fig 4E).

The opaque minerals present at a 6 cm depth consisted of abundant unaltered pyrite and abundant pseudomorphs after pyrrhotite (Fig. 4E). A few grains of unaltered chalcopyrite were observed and sphalerite was largely absent. Therefore the SAI was rated to be 4 (Fig. 3). The pseudomorphs after pyrrhotite, as observed at a 2 cm depth, consisted predominantly of marcasite. In contrast to the sub-aerial tailings, Fe (oxy)hydroxides were not associated with

these pseudomorphs. Similar to the overlying ochreous tailings, melanterite likely was previously infilling voids associated with pyrrhotite. Although melanterite was abundant in bulk XRD analysis, it was not observed in the polished thin section. Despite the fact that samples were prepared with the use of a non-aqueous lubricant, melanterite was likely dissolved or abraded during section preparation.

Energy-dispersive spectroscopic analyses of several areas of Fe oxyhydroxide solids gave results similar to those obtained at shallower depths, for example S, Si, and Al were consistently present. Samples from the 6 cm zone are the only ones in which jarosite was detected in the XRD analyses. This mineral was sparse (~1%) and was associated with the Fe (oxy)hydroxides.

Optical microscopy showed that the principal minerals at a depth of 18 cm in the submerged tailings were quartz, microcline, and albite, with amphibole and mica common. Both muscovite and biotite were present, with a small amount of the biotite replaced by chlorite or hydrobiotite, or in some cases both of these phases. Chlorite was also present as extremely fine-grained aggregates, which are interpreted to be part of the primary assemblage.

Iron oxyhydroxide phases were relatively sparse at a depth of 18 cm. Two areas of cementation were observed, but most of the (oxy)hydroxides occurred as isolated, irregular patches (Fig. 4F). Sulfide minerals consisted mainly of unaltered pyrite and pyrrhotite that exhibited varying degrees of alteration. Narrow marcasite rims surrounding preserved pyrrhotite cores were the most common form of pyrrhotite alteration. However, minor amounts of altered pyrrhotite exhibited marcasite rims and hollow cores. Numerous sphalerite grains were also observed at this depth and a relatively low SAI of 2 was assigned (Fig. 3).

The non-opaque assemblage at a depth from 20-100 cm was similar to that at 18 cm. Differences were that hydrobiotite and goethite were not detected by XRD and Fe

(oxy)hydroxides were not observed by optical microscopy. Major amounts of pyrite and pyrrhotite were present and neither mineral exhibited signs of alteration. Sphalerite was common as were lesser amounts of chalcopyrite; however, these phases comprised less than 1 vol. % of total sulfides. The SAI below 20 cm was 0 (Fig. 3).

### 4.4. Solid-phase geochemistry

Total sulfur ($S_{tot}$) concentrations from both the FX and FXS tailings exhibited similar depth dependent trends (Fig. 3). Sub-aerial tailings exhibited the greatest $S_{tot}$ depletion above the water table, whereas $S_{tot}$ depletion was limited to the upper 20 cm of the sub-aqueous tailings. These $S_{tot}$ profiles are generally in agreement with the SAI profiles. Sub-aqueous tailings showed similar $S_{tot}$ concentrations in the upper 25 cm of the core between 2001 and 2009, but showed lower concentrations with depth in 2009. Lower $S_{tot}$ concentrations in the 2009 core could be attributed to heterogeneities in mineral distribution during deposition. Total-S within unaltered tailings ranged from 16 to 28 wt.%; these values are attributed to sulfide S because primary sulfate minerals were not identified in the Fox tailings or observed in the Camp or Woods tailings impoundments (Moncur et al., 2005; 2009a; 2009b).

Total carbon (C) content was consistently low, averaging 0.04 and 0.08 wt.% for the FX and FXS tailings, respectively (Fig. 3). Total extractable carbonate contents were also low with a maximum of 0.07 wt.% in the unaltered tailings, consistent with observations in the Camp tailings. During mineralogical investigations carbonate or other carbon-bearing minerals such as graphite were not identified; therefore, it is assumed that the majority of the total C is organic carbon, which was calculated as the difference between total C and carbonate-C (Fig. 3). The highest organic C concentration was observed near the surface of both locations. The FXS tailings were vegetated, and although the organic matter was removed prior to total C analysis,

roots and other fragments of organic matter likely remained. Although the FX tailings were not vegetated, decaying organic matter (i.e., leaf litter, plant materials) was observed on the exposed tailings surface that could have contributed to the organic C content.

The order of abundance of major elements in the unaltered tailings solids, as determined by total metal concentrations, was Fe > Al > Ca > Na > Mg, on a mass basis. This order agrees with the tailings mineralogy consisting of pyrite and pyrrhotite, albite $[(Na_{0.71}Ca_{0.28}K_{0.01})_{\Sigma1.00}(Si_{2.69}Al_{1.33})_{\Sigma4.02}O_8]$, microcline $[KAlSi_3O_8]$, amphibole $[(Na_{0.48}Ca_{0.15}K_{0.06})_{\Sigma0.69}(Ca_{1.58}Fe_{0.39}Mn_{0.03})_{\Sigma2.00}(Mg_{2.51}Fe_{1.73}Al_{0.63}Ti_{0.13})_{\Sigma5.00}(Si_{6.33}Al_{1.67})_{\Sigma8.00}O_{22.93}F_{0.07}]$, and biotite $[(K_{0.91}Na_{0.02})_{\Sigma0.93}(Mg_{2.24}Fe_{0.46}Mn_{0.01}Al_{0.32}Ti_{0.03})_{\Sigma3.06}Al_{1.00}(Si_{2.80}Al_{0.20})_{\Sigma3.00}O_{10.76}F_{0.24}]$. Potassium concentrations were not measured during analyses. In general, depth dependent trends of major elements were not evident within either the FX or FXS tailings. Because sulfide oxidation reactions were not extensive enough to significantly alter Al-silicate minerals, there was minimal depletion of major elements in the ochreous zones (Fig. 5).
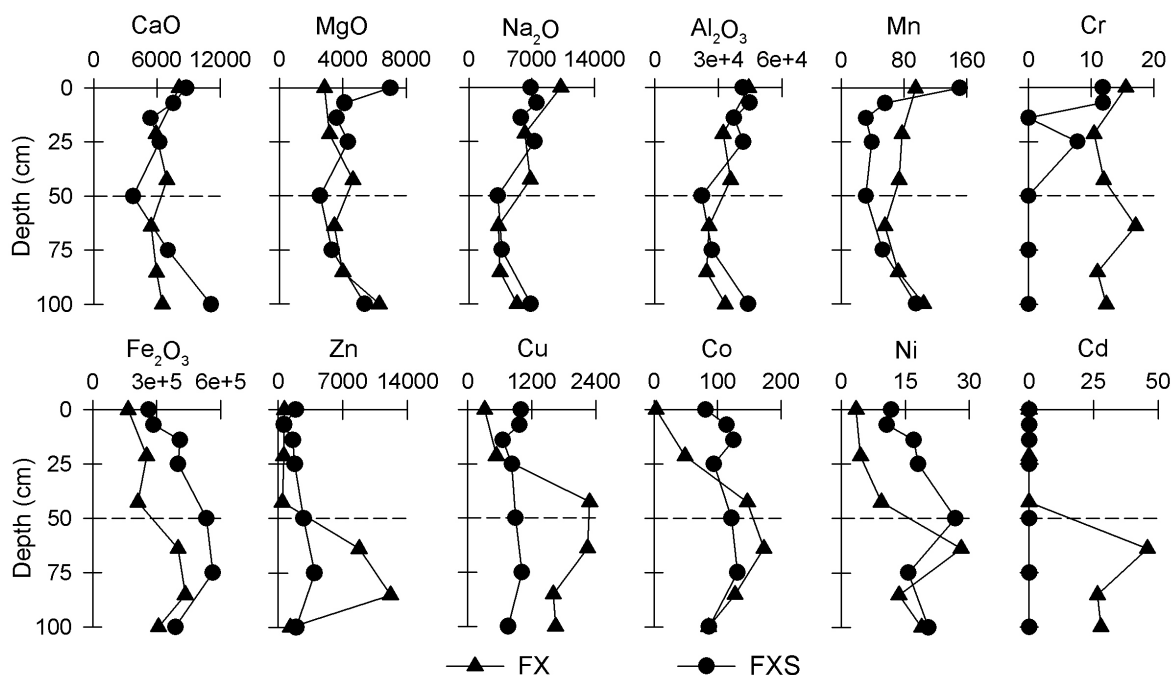
Fig. 5. Depth profile through the sub-aerial (FX) and sub-aqueous (FXS) tailings showing solid-phase concentrations of major and trace elements. Concentrations are in mg/g. The water-tailings interface is located at a depth of 0 cm for FXS and the dashed line represents the water table at FX.

The relative mass abundance of trace metals in the unaltered tailings follows the order: Zn > Cu > Mn > Co > Pb > Ni > Cr > Cd. Unlike the major elements, there is a strong depth dependent trend with Zn, Cu, Co Ni and Cd, which is consistent with assigned SAI values (Fig. 3). Within the ochreous zone of the FX tailings, Cu is depleted with concentrations increasing just above the water table, whereas the concentrations of Zn, Cd, Co and Ni have their greatest concentrations at or below the water table. This trend in is consistent with the relative resistance of sulfide minerals in oxidized tailings where chalcopyrite $[CuFeS_2]$ has the highest resistance to oxidation followed by pyrite $[(Fe,Co)S_2]$, sphalerite $[(Zn,Cd)S]$, and pyrrhotite $[(Fe,Co)_{1-x}S]$ having the least residence (Moncur et al., 2009b). The increase of Co occurred slightly higher in the profile than Zn and Cd, consistent with Co associated with pyrite, and its greater resistance to oxidation relative to sphalerite and pyrrhotite. Microprobe analysis of sphalerite grains found that Cd concentrations were consistently detected (Moncur et al., 2009b). Chromium and Mn, were not depleted in the ochreous zones because these elements were likely associated with more stable Al-silicate minerals.

### 4.5. X-ray absorption spectroscopy

Sulfur K-edge measurements for sub-aerial tailings (FX) collected from depths of 0, 20, and 40 cm exhibited a dominant peak positioned at 2472.2 eV (Fig. 6). These spectra also featured a broad hump spanning 2474 to 2480 eV and a minor peak at 2482.6 eV. Results of the LCF indicated that pyrite comprised a maximum of 8 % of the S K-edge spectrum measured for unsaturated sub-aerial tailings (Table 1). Minor chalcopyrite (4 % of S K-edge spectrum) was

present in the uppermost FX sample, whereas pyrrhotite and sphalerite were not detected. The

relatively low abundance of pyrite and chalcopyrite within these highly altered tailings is

consistent with optical examination and XRD analyses. Fitting using pyrite and marcasite

provided statistically similar results; therefore, LCF analysis could not distinguish between these

$FeS_{2(s)}$ polymorphs. Nonetheless, these results revealed that pyrite and/or marcasite were a minor

component of S K-edge spectra obtained for unsaturated tailings from the FX profile. The

absence of S associated with pyrrhotite and sphalerite is indicative of extensive sulfide-mineral

alteration, and is consistent with the assigned SAI of 9.
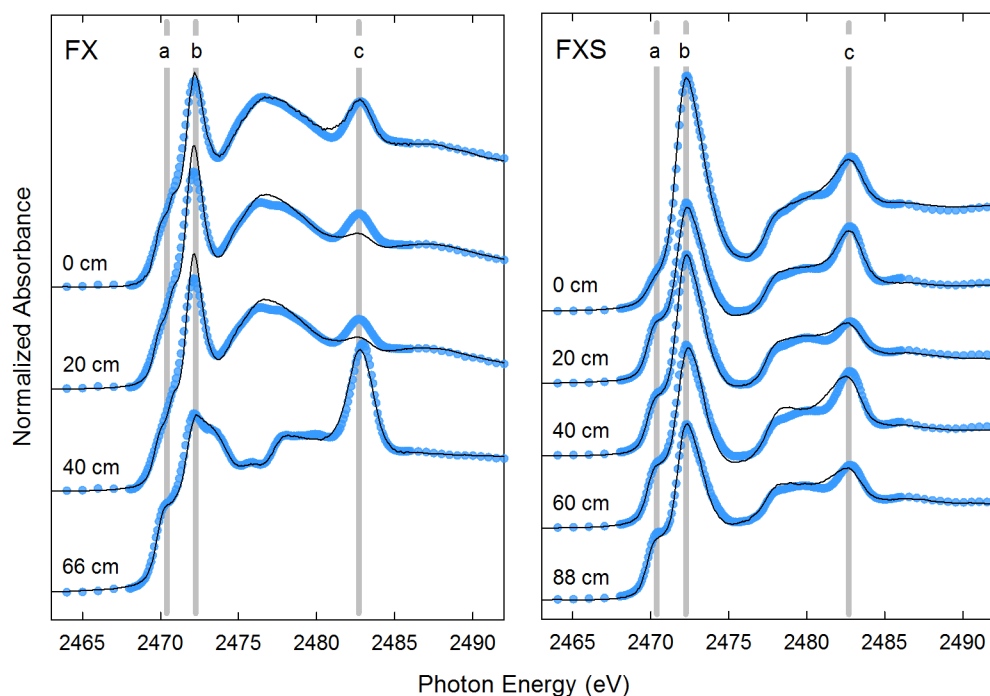


Fig. 6. Measured (line) and modeled (circles) S K-edge XANES spectra for samples of sub-aerial (FX) and sub-aqueous (FXS) tailings. Vertical shaded areas represent measured S K-edge white line maxima for (a) pyrrhotite, (b) covellite, pyrite and/or marcasite, (c) gypsum and/or jarosite reference materials.

Covellite was the dominant component of S K-edge spectra within this zone. The covellite

reference spectrum comprised 89 to 92 % of the fitted S K-edge spectra for samples obtained

from depths of 0, 20, and 40 cm. Although not detected by XRD, these LCF results suggest that covellite was likely a common phase at the sulfide grain surfaces in the unsaturated sub-aerial tailings. These apparently disparate results are attributed to methodological differences between XRD, which detects only abundant (commonly > 1 wt. % of bulk mineral assemblage) crystalline phases, and XAS, which is an element-specific method that detects both crystalline and non-crystalline phases. Moreover, the S K-edge XANES spectra were collected using TEY detection, which is highly sensitive to grain surfaces. These results therefore suggest that covellite occurred as thin surface coatings on remnant sulfides. Under oxic conditions, covellite formation may result from Cu(II) replacement of Fe(II) in pyrite (Boorman and Watson, 1976; Blowes and Jambor, 1990; Holmström et al., 1999) and/or Fe(III) leaching of chalcopyrite (Córdoba et al., 2008) under acidic pH conditions. The occurrence of covellite coatings at grain surfaces suggests that these processes have occurred in unsaturated FX tailings. The bulk ratio of pyrite and/or marcasite to covellite is likely much greater than apparent values derived from these surface sensitive S K-edge XANES analyses. Covellite is therefore interpreted as a trace phase in the bulk mineral assemblage.

Table 1. Results of LCF analysis of S K-edge XANES spectra for sub-aerial (FX) and sub-aqueous (FXS) tailings. Fitted reference spectra included pyrite (py) and marcasite (mr), pyrrhotite (po), chalcopyrite (cp), sphalerite (sp), gypsum (gp), jarosite (ja), and covellite (cv). The *R* factor is the mean-square misfit between the measured and modeled spectra.

| Location | Depth (cm) | py/ mr | po | cp | sp | gp | ja | Cv | Sum | *R* factor |
|---|---|---|---|---|---|---|---|---|---|---|
| FX | 0 | 0.06 | | 0.04 | | | | 0.89 | 1.00 | 0.0021 |
| | 20 | 0.08 | | | | | | 0.92 | 1.00 | 0.0030 |
| | 40 | 0.08 | | | | | | 0.92 | 1.00 | 0.0029 |
| | 66 | 0.49 | 0.20 | 0.24 | 0.05 | | 0.02 | | 1.00 | 0.0020 |
| FXS | 0 | 0.74 | 0.19 | | 0.02 | 0.05 | | | 1.00 | 0.0007 |
| | 20 | 0.50 | 0.30 | 0.11 | 0.04 | 0.05 | | | 1.01 | 0.0011 |
| | 40 | 0.58 | 0.29 | 0.10 | 0.04 | 0.01 | | | 1.02 | 0.0010 |
| | 60 | 0.50 | 0.38 | 0.04 | 0.04 | 0.05 | | | 1.01 | 0.0033 |
| | 88 | 0.48 | 0.20 | 0.23 | 0.05 | 0.03 | | | 1.00 | 0.0013 |

The S-K-edge XANES spectrum for the 66 cm sample differed substantially from the shallower FX sample. A peak positioned at 2472.2 eV exhibited a shoulder at approximately 2470.4 eV and an additional peak was located at 2482.8 eV. Results of LCF indicated that pyrite and/or marcasite comprised approximately 50 % of the S K-edge spectrum for this sample. Pyrrhotite, chalcopyrite, and sphalerite accounted for 20, 24, and 5 % of the S-K-edge spectrum, respectively. These results also indicate that below the water table, which was positioned 50 cm below surface, tailings have undergone considerably less oxidation than the overlying unsaturated tailings.

Sulfur K-edge XANES spectra for the sub-aqueous tailings (FXS) exhibited a dominant peak at 2473 eV (Fig. 6). Similar to the 66 cm FX sample, spectra for all FXS samples exhibited a shoulder at 2470.4 eV on the dominant peak, and a minor peak at 2482.7 eV. The LCF indicated that gypsum accounted for up to 5 % of S in the sub-aqueous tailings (Table 1). The sample obtained from the tailings-water interface (i.e., 0 cm) exhibited the smallest shoulder at

2470.4 eV, which corresponds to the S K-edge white line maximum for pyrrhotite. Pyrite plus marcasite accounted for 74 % of the S K-edge spectrum for this sample, whereas pyrrhotite and sphalerite comprised 19 %. The high ratio of pyrite-S and/or marcasite-S to pyrrhotite-S is attributed to the formation of secondary marcasite rims at pyrrhotite surfaces. Additionally, the relatively low abundance of sphalerite is consistent with optical mineralogy.

All deeper FXS samples (i.e., 20, 40, 60 and 88 cm) were characterized by similar S K-edge spectra. Results of LCF revealed that 48 to 58 % of the S K-edge spectra were contributed by pyrite and/or marcasite. Pyrrhotite and chalcopyrite accounted for an additional 20 to 38 % and 4 to 23 % of the S K-edge spectra, respectively. Minor amounts of sphalerite and gypsum also were also present in these samples. These results are generally consistent with results of XRD analysis and optical examination of unaltered tailings.

### 4.6. Pore-water chemistry

#### 4.6.1. Sub-aerial tailings

Pore water was squeezed from core at 25 cm intervals from surface to a 100 cm depth from the land-based tailings in 2001 and 2009. The oxidation of sulfide minerals within the vadose zone of the tailings has resulted in generation of low pH conditions (pH 1.9 to 3.7) and elevated concentrations of dissolved $SO_4$ (up to 59,000 mg/L), Fe (up to 28,000 mg/L) and trace metals (Fig. 7). The highest concentrations of dissolved metals were observed near the tailings surface although elevated concentrations of dissolved Fe, $SO_4$ and other metals persisted through the water table to a depth of 100 cm (Table 2).
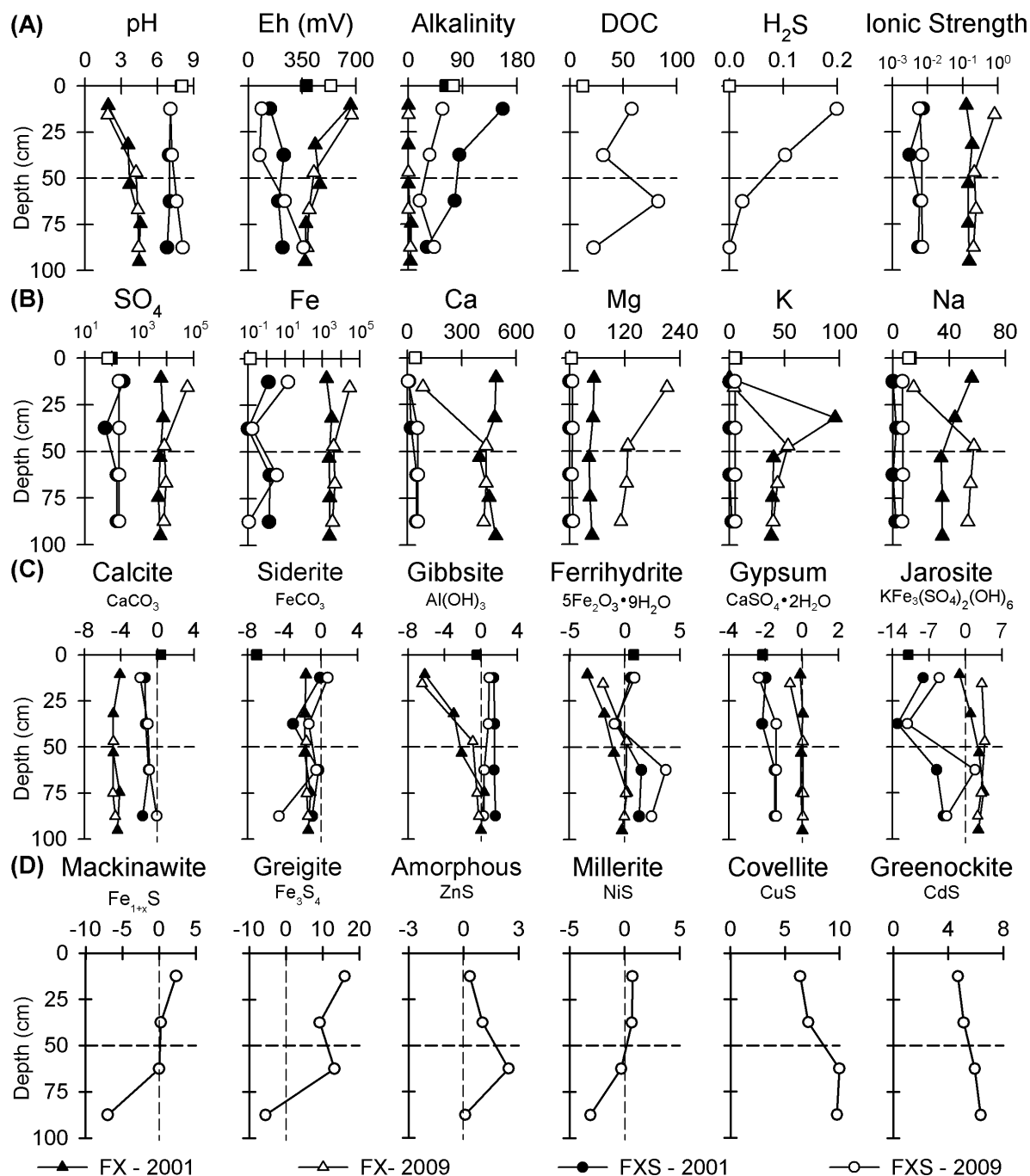
Fig. 7. Depth profiles through the land-based (FX) and submerged (FXS) tailings; (A) and (B) showing pore-water chemistry and calculated ionic strength; (C) and (D) showing calculated saturation indices. All concentrations are in mg/L except where noted. Dashed line represents water table location in the FX. The Fox Lake (FL) water-tailings interface of FXS is shown as a depth of 0 cm.

Depth profiles of pH and Eh values were consistent over the eight year period between 2001 and 2009. However, an order of magnitude increase of sulfate, chloride and most dissolved metals occurred at a depth of 15 cm in 2009 (Fig. 7). For example, between 2001 and 2009, $SO_4$ and Fe increased from 6,000 to 59,000 mg/L and 2,000 and 28,000 mg/L, respectively (Table 2). The elevated concentrations of dissolved $SO_4$ and metals at a depth of 15 cm in 2009 resulted in much higher calculated ionic strength values. This increase of dissolved elements is a result of continuing sulfide oxidation reactions occurring in the near-surface tailings over the eight-year period. Alkalinity was not detected in pore-water in the vadose zone of the land-based tailings. In 2001, alkalinity values were minimal; 5 mg/L (as $CaCO_3$) at 75 cm and 3 mg/L (as $CaCO_3$) at 95 cm below the surface. By 2009, the only measureable alkalinity was 3 mg/L, at a depth of 90 cm below surface. At and below the water table, concentrations of dissolved ions were relatively similar. Modeled saturation indices indicated that tailings pore waters were undersaturated with respect to carbonate minerals (Fig. 7). Pore water was undersaturated with respect to Al-hydroxide and Fe(III) (oxy)hydroxide mineral phases, but become supersaturated with respect these phases near the water table. The pore-water was supersaturated with respect to goethite throughout the depth profile. Low temperature mine waters are typically supersaturated with respect to goethite when other Fe(III) (oxy)hydroxide are also at saturation. As a result, this observation is not necessarily indicative of goethite precipitation (Alpers and Nordstrom, 1999). However, goethite was the only Fe oxyhydroxide consistently detected in all X-ray diffractograms examined from the FX tailings samples, in agreement with modeling results. The pore water was also at saturation with respect to gypsum and jarosite suggesting that these secondary mineral phases could be controlling dissolved concentrations of $SO_4$, Fe and K.

Table 2. Pore water chemistry measured from the land-based (FX) and submerged (FXS) tailings in 2001 and 2009.

| Location | pH | $SO_4$ mg/L | Fe mg/L | Al mg/L | Zn mg/L | Cu mg/L | Cr mg/L | Co mg/L | Cd mg/L |
|---|---|---|---|---|---|---|---|---|---|
| **0.13 m depth** | | | | | | | | | |
| FX-2001 | 1.93 | 6200 | 1600 | 190 | 9.3 | 6.4 | 0.21 | 0.36 | 0.13 |
| FX-2009 | 1.90 | 59000 | 28000 | 1500 | 170 | 170 | 0.63 | 33 | 3.3 |
| FXS-2001 | 7.09 | 260 | 1.26 | <dl | <dl | 0.01 | <dl | <dl | <dl |
| FXS-2009 | 7.05 | 1600 | 1.33 | 0.01 | 0.07 | 2.2 | <dl | 0.0006 | 0.0006 |
| **0.62 m depth** | | | | | | | | | |
| FX-2001 | 3.71 | 5800 | 2200 | 14 | 7.0 | 0.08 | 0.09 | <dl | 0.16 |
| FX-2009 | 4.38 | 9400 | 4500 | 68 | 7.0 | 19 | 0.05 | 0.1 | 0.39 |
| FXS-2001 | 7.04 | 150 | 1.54 | <dl | 0.01 | 0.01 | <dl | 0.006 | <dl |
| FXS-2009 | 7.15 | 1700 | 0.16 | 0.04 | 0.07 | 0.9 | <dl | 0.0003 | <dl |
| **0.89 m depth** | | | | | | | | | |
| FX-2001 | 4.49 | 5900 | 2400 | 8.3 | 2.2 | <dl | 0.08 | 0.05 | 0.16 |
| FX-2009 | 4.43 | 7900 | 3500 | 68 | 15 | 16 | 0.02 | 0.3 | 0.02 |
| FXS-2001 | 6.81 | 150 | 1.34 | <dl | 0.01 | 0.01 | <dl | <dl | <dl |
| FXS-2009 | 7.00 | 1700 | 1.35 | 0.01 | 0.06 | <dl | <dl | 0.0003 | <dl |
| dl | 0.01 | <0.01 | <0.0002 | < 0.01 | <0.0005 | <0.0005 | <0.0005 | <0.0005 | <0.0005 |

## 4.6.2. Sub-aqueous tailings

In contrast to the sub-aerial tailings, pore water from the sub-aqueous tailings was at circumneutral pH and mildly reducing, containing low concentrations of $SO_4$ and Fe. Most dissolved metal concentrations were near or below analytical detection limits (Table 2). Concentrations of dissolved ions, pH, Eh and calculate ionic strength exhibited minimal variability between 2001 and 2009 (Fig. 7). However, alkalinity concentrations measured in 2009 were almost twice as high as those measured in 2001. Speciation modeling results shows that pore waters approached or attained saturation with respect to calcite and siderite, suggesting that equilibrium with respect to these carbonate minerals may be maintaining circumneutral pH condition (Blowes et al., 2013). Other minerals at saturation or supersaturation in pore-waters that might be controlling dissolved ions include gibbsite, ferrihydrite, goethite, gypsum and jarosite (Fig. S1).

## 4.7. Sulfate reduction

Values of $\delta^{34}S$ and $\delta^{18}O$ for dissolved sulfate were determined for pore water from the sub-aerial and sub-aqueous tailings, and for surface water from Fox Lake. Values of $\delta^{34}S_{SO4}$ for the sub-aerial tailings exhibited little variation (1.8 to 3.3 ‰) and were consistent with $\delta^{34}S$ values of the primary sulfide minerals, which ranged from 0.2 to 2.6 ‰ ($n = 7$; Moncur et al., 2009a). Fractionation between $\delta^{34}S$ in the primary sulfide and associated dissolved sulfate was less than 2 ‰ (Taylor et al., 1984; Rye et al., 1992).
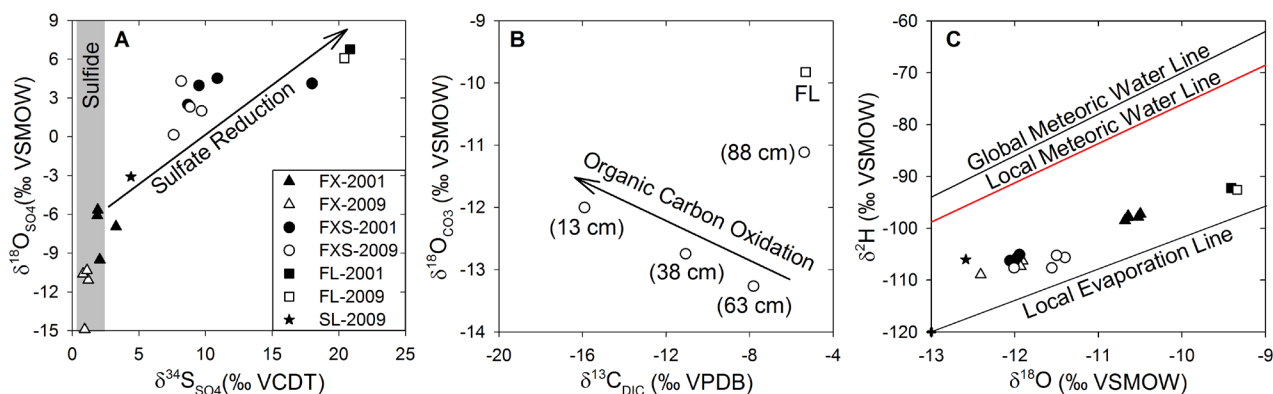


Fig. 8. (A) Plot of $\delta^{34}S$ versus $\delta^{18}O_{SO4}$ values of dissolved sulfate from sub-aerial tailings (FX), sub-aqueous tailings (FXS), Fox Lake (FL) and Sherlett Lake (SL) surface water. The shaded area represents the range of $\delta^{34}S$ values measured from seven primary sulfide minerals. VSMOW - Vienna Standard Mean Ocean Water; VCDT – Vienna Canyon Diablo Troilite. (B) Plot of $\delta^{13}C_{DIC}$ versus $\delta^{18}O_{CO3}$ values measured in 2009 from FXS and FL. Values in brackets refer to sample depths below water-tailings interface. VPDB – Vienna Pee Dee Belemnite (C) Plot of $\delta^{18}O$ versus $\delta^2H$ values measured in 2001 and 2009 from FX, FXS, FL and SL.

Values of $\delta^{34}S$ and $\delta^{18}O$ for dissolved $SO_4$ for the sub-aqueous tailings were generally more positive than the primary sulfide minerals, which is consistent with the fractionation associated with bacterial (dissimilatory) $SO_4$ reduction (Fig. 8A). The $\delta^{34}S_{SO4}$ values in the sub-aqueous tailings ranged from 18 ‰ (13 cm depth) to 7.6 ‰ (63 cm depth). Similarly, $\delta^{18}O_{SO4}$ values ranged from 4.1 ‰ (13 cm depth) to 0.2 ‰ (63 cm depth). Decreases in $SO_4$ concentrations resulting from dissimilatory sulfate reduction (DSR) can generate significant sulfur isotope

fractionation where the remaining $SO_4$ becomes enriched in $^{34}S$ (Harrison and Thode, 1958; Kaplan and Rittenberg, 1964; Fritz et al., 1989; Habicht and Canfield, 1997; Knöller et al, 2004). Sulfate reduction was also apparent from other geochemical parameters measured for the submerged tailings and for Fox Lake. As sulfate-reducing bacteria catalyze the oxidation of organic carbon, the reduction of $SO_4$ to $H_2S$ (Berner, 1980) occurs through the reaction:

$$SO_4^{2-} + 2CH_2O \rightarrow H_2S + 2HCO_3^- \tag{1}$$

where $CH_2O$ represents a generic organic compound. The organic carbon source in Fox Lake and the submerged tailings likely originated from overlying vegetation and DOC in the surface waters. (Fig. 4). The precipitation of sparingly-soluble metal-sulfides occurs when $H_2S$ is produced in the presence of dissolved metals:

$$Me^{2+} + S^{2-} \rightarrow MeS \tag{2}$$

where $Me^{2+}$ denotes a divalent metal such as Fe, Cd, Ni, Cu, Co and Zn; and MeS represents the corresponding metal sulfide precipitate (Berner, 1985; Seal, 2003). The sequence of reactions in equations (1) and (2) decreases the concentrations of dissolved $SO_4$, Fe, and other metals, and increases pore-water alkalinity and pH (Tuttle et al., 1969; Benner et al., 1999; Lindsay et al., 2009b). The reduction of $SO_4$ described in reaction (1) is consistent with the trends of increased pH, alkalinity, and $H_2S$, and with the decreased Eh observed in the sub-aqueous tailings pore-water (Fig.7 ). Studies on acid neutralization of lakes (Cook et al., 1986), tailings (Benner et al., 2000), tailings amended with organic substrate (Lindsay et al., 2011) and for the treatment of acid rock drainage (Benner et al., 1999) have shown that DSR coupled with secondary metal-sulfide precipitation can promote increased concentrations of alkalinity, pH buffering, and the formation of secondary metal-sulfide phases.

Values of $\delta^{13}C_{DIC}$ became more negative towards the tailings surface while, with the exception of the 88 cm sample, values of $\delta^{18}O_{CO3}$ became more positive (Fig. 8B). These trends in $\delta^{13}C_{DIC}$ and $\delta^{18}O_{CO3}$ are generally consistent with DSR coupled with oxidation of organic carbon. The pore-water sample with highest concentration of $H_2S$, alkalinity and most enriched $\delta^{34}S_{SO4,}$ $\delta^{18}O_{SO4}$ and $\delta^{18}O_{CO3}$ and depleted $\delta^{13}C_{DIC}$ is near the interface with the overlying water column, where the highest concentrations of organic carbon occurred in the sediments (Fig. 3). Depth profiles of alkalinity for the sub-aqueous tailings (FXS, Fig. 7) generally decrease from the tailings surface, with the shallowest depths having alkalinity concentrations that are similar the values measured in Fox Lake. However, mixing of Fox Lake water and tailings pore water (13 cm depth) cannot account for observed differences in the $\delta^{13}C$-DIC and $\delta^{18}O_{CO3}$ (Fig. 8B). These observations are consistent with the interpretation that DSR occurred within the sub-aqueous tailings and that rates may have been greatest immediately below the water-tailings interface.

The $\delta^{18}O$ and $\delta^{2}H$ composition of pore water in the sub-aerial and sub-aqueous tailings reveal temporal and spatial differences in water sources. In 2001, pore-water from the sub-aerial and sub-aqueous tailings, and from the Fox Lake were all distinct and plotted along a local evaporation line (Gibson et al., 2010). Pore-water from the sub-aqueous tailings exhibited the most negative $\delta^{18}O$ and $\delta^{2}H$ values, whereas pore water from the sub-aerial tailings was characterized by slightly enriched $\delta^{18}O$ and $\delta^{2}H$ values. The sub-aerial tailings pore water exhibited more negative $\delta^{18}O$ and $\delta^{2}H$ values in 2009 compared to 2001. These values were also more negative relative to sub-aqueous tailings pore-water collected in 2009. Variations in $\delta^{18}O$ and $\delta^{2}H$ values between the sampling events were relatively small for the submerged tailings, indicating a fairly consistent stable hydrological setting. The sub-aerial tailings pore-water

exhibited a larger range in $\delta^{18}O$ and $\delta^2H$ compositions between the two sampling events, indicating variations in the source of water or in the degree of evaporation. Pore water collected in 2001 from the sub-aerial tailings exhibited more enriched isotopic signatures than in 2009, suggesting greater evaporation, or mixing with summer precipitation or enriched surface water. The apparent lack of hydrological variability in the sub-aqueous tailings is consistent with observed stability of the geochemical profiles over time. In contrast, the sub-aerial tailings exhibited greater geochemical variability, which may be attributed, at least in part, to greater hydrological variability as suggested by these $\delta^{18}O$ and $\delta^2H$ values. The weighted mean annual composited of local precipitation for the areas was -17‰ for $\delta^{18}O$ and -130‰ for $\delta^2H$, measured in The Pas, MB, the nearest long-term precipitation monitoring station, 150 km south of Sherridon. Local groundwater is typically similar to the weighted mean annual composited of local precipitation, with Canada being more bias towards winter precipitation (Jasechko et al., 2014). The LEL of the area is from a survey of 151 lakes in northwestern Manitoba (Gibson et al. 2010) and the intercept of the LEL for NW Manitoba and the GMWL (Fritz eta al., 1987) is about -17‰. Mixing of groundwater ($\delta^{18}O$ of -17‰) with Fox Lake water ($\delta^{18}O$ of -9.5) suggests that porewater from the FXS tailings ($\delta^{18}O$ of -11.5) was comprised of more than 50% surface water.

Modeled saturation indices indicate that pore water from the sub-aqueous tailings approached saturation or became supersaturated with respect to secondary sulfide minerals (Fig. 7). Speciation modeling results were consistent with the presence of secondary sulfides observed in the submerged tailings at a depth of 6 cm. Secondary grains of covellite, each no more than 15 μm across, occur within the pyrrhotite pseudomorphs. In addition, rims of secondary marcasite on unaltered primary pyrite were also identified at a depth of 6 cm in the submerged

tailings. The rims occurred on a few grains and were extremely thin (Fig. 9). The optical identification of the rims as marcasite was consistent with EDS analysis. Secondary metal-sulfide phases were not detected in the S K-edge XANES spectra from the sub-aqueous tailings. However, similar to the XRD results, these phases were likely below method detection limits in the presence of abundant pyrite and pyrrhotite (Table 1). Furthermore, despite the textural difference between the host pyrite and the fine-grained marcasite rim, the two were difficult to distinguish in backscattered-electron images because both minerals had the same composition. Other studies (e.g., Pedersen et al., 1993; Paktunc and Davé, 2002; Lindsay et al., 2011) have also reported the presence of secondary sulfide minerals, which control metal and sulfate concentrations in sulfate-reducing zones at mining-impacted sites.
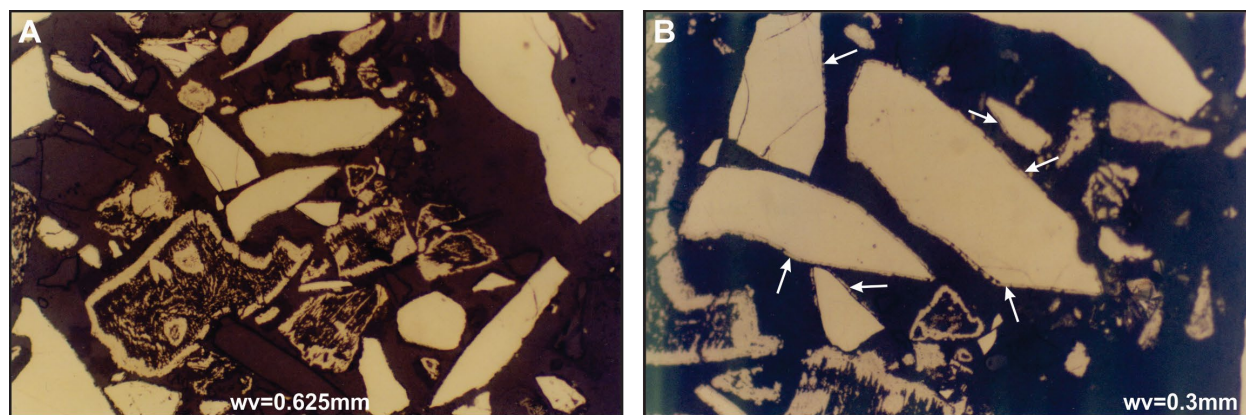


Fig. 9. Photomicrographs of sub-aqueous tailings at a 6 cm depth in plain reflected light showing (A) unaltered grains of pyrite with thin rims of secondary marcasite, near center of image. (B) Enlargement of (A) with arrows showing the narrow rims of secondary marcasite on the primary pyrite grains. Width of view is represented by wv.

## 4.8. Microbial enumerations

Most-probable number populations of IRB and SRB were low within the ochreous zone of the sub-aerial tailings, which was dominated by aSOB. Populations of nSOB were consistently low throughout the sub-aerial tailings profile. Decreasing populations of aSOB with depth in the sub-aerial tailings corresponded to an increase in SRB numbers below the ochreous zone. This

trend is indicative of $O_2$ consumption due to sulfide-mineral oxidation above the water table and DSR in the underlying saturated anoxic zone. Fermenters (APB) were not detected in the FX profile and IRB numbers above the detection limit were attributed to false positives associated with high dissolved Fe(II) concentrations (Fig. 10).

In contrast to the sub-aerial tailings, nSOB exhibited higher MPN populations than aSOB in the sub-aqueous tailings. Nonetheless, populations of both nSOB and aSOB were low at depths greater than 13 cm below the tailings surface. The largest populations of SRB and IRB within the sub-aqueous tailings occurred near the water-tailings interface. These values also corresponded to the highest APB numbers, which suggests that the production of organic acids via fermentation supported SRB and IRB activity at this depth (Lindsay et al., 2011; MacDonald et al., 2013). Rapid consumption of these organic acids by SRB and IRB could explain why DOC concentrations (Fig. 10) were not substantially higher near the water-tailings interface, where active DSR may have been occurring (McDonald et al., 2013). Populations of SRB and IRB generally decreased with depth, yet viable populations of these heterotrophic bacteria persisted throughout the sub-aqueous tailings profile. The large shift in the $\delta^{34}S_{SO4}$ values and an increase of $H_2S$ concentration and SRB population indicate that active DSR was occurring in the sub-aqueous tailings.
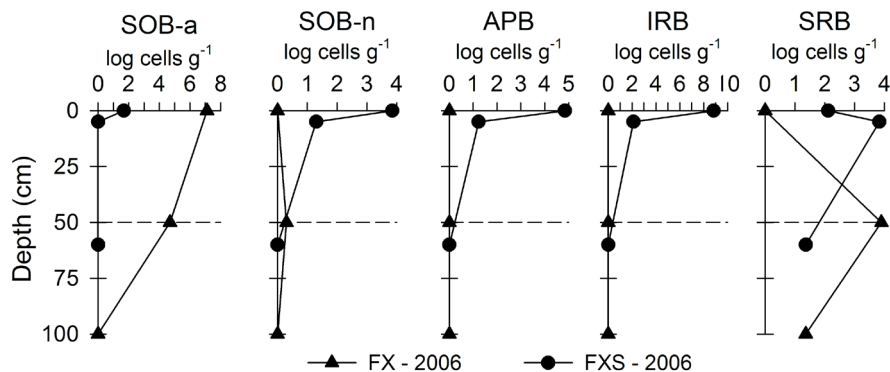
Fig. 10. Most probable number (MPN) populations of acidophilic S-oxidizing bacteria (aSOB), neutrophilic S-oxidizing bacteria (nSOB), acid-producing (fermentative) bacteria (APB), iron-reducing bacteria (IRB) and $SO_4$-reducing bacteria (SRB) in the land-based (FX) and submerged (FXS) tailings. The water-tailings interface is located at a depth of 0 cm for FXS and the dashed line represents the water table at FX.

### 4.9. Fox Lake water quality

Comparison of water quality parameters for the submerged tailings, land-based tailings and Fox Lake (Fig. 7) shows the importance of limiting oxidation to minimize the generation of low pH waters with high dissolved metal concentrations. Despite low pH, high $SO_4$ and metal concentrations present in pore-water of the land-based tailings, the water quality of Fox Lake remained circumneutral, likely due to the ameliorating influence of DSR (Table 3). The lake surface water was at equilibrium with respect to calcite suggesting this phase may be controlling the pore-water pH (Fig. 7). The $\delta^{18}O$ and $\delta^2H$ composition of Fox Lake is indicative of evaporative enrichment in a surface water body, and suggest hydrological changes were minimal between sampling campaigns. The $\delta^{34}S_{SO4}$ and $\delta^{18}O_{SO4}$ values were consistent with the dissolved $SO_4$ being strongly influenced by DSR. Water-quality data are sparse prior to 2001, but the limited data available seems to indicate a general improvement in water quality over the 25-year period (Table 3).

Table 3. Water chemistry measured from Fox Lake (FL) surface water between 1983 and 2009. Median calculations for FL and Sherlett Lake (SL) were determined from 2002 to 2009 data. GPAL refers to the Canadian guidelines for the protection of aquatic life (CCME, 2007). Historical values from Beck[a] (1983) and Beck[b] (1988). Detection limit represented by dl. Hyphens indicate that parameter was not determined.

| Date | pH | Alkalinity mg/L CaCO$_3$ | SO$_4$ mg/L | Fe mg/L | Zn mg/L | Cu mg/L | Ca mg/L | Mg mg/L |
|---|---|---|---|---|---|---|---|---|
| 1983[a] | 7.3 | - | - | - | 0.26 | 0.56 | - | - |
| 1988[b] | 7.2 | 48 | - | 1 | 0.5 | 0.01 | 64 | 5.7 |
| 2001 | 7.97 | 62 | 93 | 0.09 | <dl | 0.005 | 45 | 4.5 |
| 2002 | 8.44 | 57 | 33 | <dl | <dl | <dl | 47 | 4.6 |
| 2003 | 7.79 | 68 | 81 | 0.38 | <dl | 0.003 | 42 | 4.4 |
| 2004 | 7.34 | 88 | 84 | 0.19 | <dl | 0.006 | 52 | 4.9 |
| 2005 | 7.53 | 86 | 70 | 1.0 | 0.005 | <dl | 47 | 4.6 |
| 2006 | 8.56 | 70 | - | - | - | - | - | - |
| 2008 | 7.90 | 58 | 72 | 0.06 | 0.002 | 0.003 | 41 | 4.2 |
| 2009 | 8.05 | 75 | 70 | 0.13 | 0.002 | <dl | 44 | 4.6 |
| FL Median | 7.9 | 72 | 70 | 0.16 | 0.002 | 0.003 | 45 | 4.6 |
| SL Median | 7.6 | 25 | 4.5 | 0.10 | 0.10 | 0.002 | 7.6 | 2.8 |
| GPAL | 6.5-9.0 | - | - | 0.3 | 0.03 | 0.002 | - | - |
| dl | 0.01 | <1 | <0.01 | <0.0002 | <0.0005 | <0.0005 | <0.005 | <0.0001 |

Sherlett Lake is a shield lake located up-stream of the former mining site and is therefore considered representative of background water quality (Beck, 1983; Moncur et al., 2014). Sherlett Lake was sampled annually between 2002 and 2009. A comparison of water quality between Fox Lake and Sherlett Lake indicated that dissolved Fe and Cu concentrations were similar; however, Fox Lake exhibited much lower dissolved Zn concentrations (Table 3). Elevated dissolved Zn concentrations observed in Sherlett Lake are related to weathering of sulfide-bearing waste rock from the mine that was used as construction along the shore (Moncur et al., 2014). Conversely, dissolved SO$_4$, Ca and Mg concentrations were an order of magnitude higher in Fox Lake than Sherlett Lake, likely a result of (sulfide) mineral weathering products from the sub-aerial tailings. The $\delta^{18}$O and $\delta^2$H composition of Sherlett Lake, -12.59 ‰ and -106.1 ‰, respectively, shows less evaporative enrichment then Fox Lake ($\delta^{18}$O: -9.34 ‰ and $\delta^2$H: -92.6 ‰), typical of a flow-through surface-water body as described by Moncur et al. (2014). The $\delta^{34}$S-SO$_4$ value measured for Fox Lake in 2009 (20.4 ‰) was indicative strong

fractionation via DSR, whereas the $\delta^{34}S_{SO4}$ value for Sherlett Lake (4.4 ‰) was more representative of sulfide-mineral oxidation (Fig. 8). Strong reducing conditions in Fox Lake are likely controlling dissolved metals concentration in the surface waters, nevertheless weathering of the sub-aerial tailings is evident from the elevated dissolved concentrations of $SO_4$, Ca, and Mg. Dissolved Fe, Zn, and Cu concentrations remained below Canadian maximum concentrations for the protection of aquatic life (CCME, 2007).

## 5. Conclusions

Sulfide mine tailings were deposited into Fox Lake more than 60 years ago. This deposit included sub-aerial tailings (FX) exposed to atmospheric oxygen since deposition and sub-aqueous tailings (FXS) positioned below a continuous 100 cm water cover. The sub-aerial tailings exhibited a well-defined, ochreous oxidation zone with extensive sulfide mineral depletion that extended from surface to about 40 cm depth. A transitional zone of much weaker oxidation extended from 40 to 60 cm below the tailings surface, and the sulfide mineral assemblage remained unaltered at depths > 60 cm. In contrast to the sub-aerial tailings, the oxidation zone observed in the sub-aqueous tailings was thin, extending < 6 cm below the water-tailings interface.

Pore water collected from the sub-aerial tailings exhibited low pH, depleted alkalinity, and elevated concentrations of dissolved $SO_4$ and metals (i.e., Fe, Zn, Cu). The sub-aerial tailings contained elevated populations of acidophilic sulfur oxidizing bacteria (aSOB), which catalyze sulfide-mineral oxidation at low pH in the presence of $O_2$ and water. Increased populations of sulfate-reducing bacteria (SRB) below the ochreous zone were indicative of $O_2$ consumption via sulfide-mineral oxidation in the overlying tailings. Conversely, the sub-aqueous tailings exhibited strong reducing conditions with pore-water characterized by circumneutral pH and low

concentrations of dissolved $SO_4$ and metals. This pore water also exhibited elevated $H_2S$ concentrations and strong $\delta^{34}S_{SO4}$ enrichment indicative of dissimilatory sulfate reduction (DSR) whereas the subaerial tailings porewater had depleted $\delta^{34}S_{SO4}$ values similar to the signature of sulfide minerals in the tailings. Marcasite occurred as secondary coatings on primary minerals within 2 cm of sub-aqueous tailings surface. Secondary covellite was also observed in this zone. These findings further emphasize the influence of reducing conditions and microbial activity on metal mobility within sub-aqueous mine tailings. Results from this study suggest that the use of sub-aqueous tailings deposition as an approach to limiting oxidation may be effective over extended time periods.

## References

Allison, J.D., Brown, D.S., Nova-Gardac, K.L., 1990. MINTEQA2/PRODEFA2, A Geochemical Assessment Model for Environmental Systems, Version 3.0 User's Manual. Environmental Research Laboratory, Office of Research and Development, U.S. EPA, Athens, GA.

Alpers, C .N., Nordstrom, D. K., 1999. Geochemical modeling of water-rock interactions in mining environments. In: Plumlee, G.S., Logsdon, M.J. (Eds.). Reviews in Economic Geology, vol. 6A . The Environmental Geochemistry of Mineral Deposits, Part A, Processes, Methods and Health Issues, 289-324.

Assayag, N., Rivé, K., Ader, M., Jézéquel, D., Agrinier, P., 2006. Improved method for isotopic quantitative analysis of dissolved inorganic carbon in natural water samples. Rapid Commun. Mass Spectrom. 20, 2243-2251.

Awoh, A.S., Mbonimpa, M., Bussière, B., 2013. Determination of the reaction rate coefficient of sulphide mine tailings deposited under water J. Environ. Manage. 128, 1023-1032.

Ball, J.W., Nordstrom, D.K., 1991. User's manual for WATEQ4F with revised thermodynamic data base and test cases for calculating speciation of major, trace and redox elements in natural waters. U.S. Geol. Surv. Open-File Rep. 91-183.

Barker, J.F., Chatten, S., 1982. A technique for determining low concentrations of total carbonate in geological materials. Chem. Geol. 36, 317-323.

Beck, A.E., 1983. Aquatic impact assessment of the Sherridon mine. Water Standards and Studies Report #83-25.

Beck, A.E., 1988. Memorandum report: Data report and summary for data collected during 1988. Manitoba Environmental Management Division.

Benner, S.G., Blowes, D.W., Gould, W.D., Herbert, R.B., Ptacek, C.J., 1999. Geochemistry of a permeable reactive barrier for metals and acid mine drainage. Environ. Sci. Technol. 33, 2793-27997.

Benner, S.G., Gould, W.D., Blowes, D.W., 2000. Microbial populations associated with the generation and treatment of acid mine drainage. Chem. Geol. 169, 435- 448.

Berner, R.A., 1980. Early Diagenesis: A Theoretical Approach. Princeton University Press, Princeton, NJ.

Berner, R.A., 1985. Sedimentary pyrite formation: an update. Geochim. Cosmochim. Acta 48, 605-615.

Blowes, D.W., Jambor, J.L., 1990. The pore-water chemistry and the mineralogy of the vadose zone of sulfide tailings, Waite Amulet, Quebec. Appl. Geochem. 5, 327-346.

Blowes, D.W., Al, T.A., Lortie, L., Gould, W.D., Jambor, J.L., 1996. Microbiological, chemical, and mineralogical characterization of the Kidd Creek mine tailings impoundment, Timmins area, Ontario. Geomicrobiol. J. 13, 13–31.

Blowes, D.W., Ptacek, C.J., Jambor, J.L., Weisener, C.G., Paktunc, D., Gould, W.D., Johnson, D.B., 2013. The geochemistry of acid mine drainage. In: Lollar, B.S., Holland, H.D., Turekian, K.K. (Eds.), Environmental Geochemistry. Treatise on Geochemistry, vol. 9, second ed. Elsevier-Pergamon, Oxford.

Boorman, R.S., Watson, D.M., 1976. Chemical processes in abandoned sulphide tailings dumps and environmental implications for Northeastern New Brunswick. CIM Bull. 69, 89-96.

Broman, P.G., Haglund P. Mattsson, E., 1991. Use of sludge for sealing purposes in dry covers-Development and field experiences. In :Second Internat. Conf. Abatement Acidic Drainage Vol. 1, MEND Secretariat, Ottawa, Ontario. pp. 515-528.

CCME (Canadian Council of Minister of the Environment), 2007. Canadian water quality guidelines for the protection of aquatic life: summary table. In: Canadian Environmental Quality Guidelines, 1999, Canadian Council of Ministers of the Environment, Winnipeg.

Chou, I.M., Seal, R.R., Wang, A., 2013. The stability of sulfate and hydrated sulfate minerals near ambient conditions and their significance in environmental and planetary sciences. J Asian Earth Sci. 62, 734-758.

Córdoba, E.M., Muñoz, J.A., Blázquez, M.L., González, F., Ballester, A., 2008. Leaching of chalcopyrite with ferric ion. Part II: Effect of redox potential. Hydrometallurgy 93, 88–96.

Davé, N.K., Lim, T.P., Horne, D., Boucher, Y., Stuparyk, R., 1997. Water cover on reactive tailings and wasterock: Laboratory studies of oxidation and metal release characteristics. In: 4th International Conference on Acid Mine Drainage, May 31eJune 6, Vancouver, pp. 779-794.

Dobchuk, B., Nichol, C., Wilson, G.W., Aubertin, M., 2013. Evaluation of a single-layer desulphurized tailings cover. Can. Geotech. J. 50, 777-792.

Elberling, B., Damgaard, L.R., 2001. Microscale measurements of oxygen diffusion and consumption in subaqueous sulphide tailings. Geochim. Cosmochim. Acta 65, 1897-1905.

Environment Canada, 2012. Canadian Climate Normals, 1927-2012, Flin Flon, Manitoba. <http://climate.weatheroffice.ec.gc.ca/Welcome_ehtml>

Farley, W.J., 1949. Geology of the Sherritt Gordon Ore Body. CIM Bull. 42, 25-30.

Freeze, R.A., Cherry, J.C., 1979. Groundwater. Prentice Hall, Englewood Cliffs, New Jersey.

Fritz, P., Drimmie, R.J., Frape, S.K., O'Shea, K.J., 1987. The isotopic composition of precipitation and groundwater in Canada. Isotope Techniques in Water Resources Development, International Atomic Energy Agency, Vienna, IAEA-SM-299/17, pp. 539-550.

Froese, E., Goetz, P.A., 1981. Geology of the Sherridon Group in the vicinity of Sherridon, Manitoba. Geol. Surv. Can. Pap., pp. 80-21.

Gibson, J.J.,  Birks, S.J., Jeffries, D.S., Kumar, S., Scott, K.A., Aherne, J., Patrick D. Shaw, P.D., 2010. Site specific estimates of water yield applied in regional acid sensitivity surveys across western Canada. J. Limnol. 69, 67-76.

Giesemann, A., Jäger, H.J., Norman, A.-L., Krouse, H.R., Brand, W.A., 1994. On-line sulfur-isotope determination using an elemental analyzer coupled to a mass spectrometer. Anal. Chem. 66, 2816–2819.

Goetz, P.A., Froese, E., 1982. The Sherritt Gordon massive sulfide deposit. Precambrian Sulfide Deposits, H.S. Robinson Memorial Volume. Hutchinson, R.W., Spence, C.D., and Franklin, J.M (Eds.). Geol. Assoc. Can. Special Pap. 25, pp. 557-569.

Gould, W.D., Stitchbury, M., Francis, M., Lortie, L., Blowes, D.W., 2003. An MPN method for the enumeration of iron-reducing bacteria. In: Spiers, G., Beckett, P., Conroy, H. (Eds.), Proceedings of Sudbury '03, Mining and the Environment III. Laurentian University, Sudbury, ON, pp. 153–157.

Gunsinger, M.R., Ptacek, C.J., Blowes, D.W., Jambor, J.L., 2006. Evaluation of long-term sulphide oxidation processes within pyrrhotite tailings, Lynn Lake, Manitoba. J. Contam. Hydrol. 83, 149-170.

Habicht, K.S., Canfield, D.E., 1997. Sulfur isotope fractionation during bacterial sulfate reduction in organic-rich sediments. Geochim. Cosmochim. Acta. 61, 5351– 5361.

Hamilton, R., Fraser, W.W., 1978. A case history of natural underwater revegetation: Mandy Mine high sulfide tailings. Reclam. Rev. 1, 61-65.

Harrison, A.G., Thode, H.G., 1958. Mechanism of the bacterial reduction of sulphate from isotope fractionation studies. Trans. Faraday Soc. 54, 84–92.

Herbert, R.B., Jr., Benner, S.G., Blowes, D.W., 2000. Solid-phase iron-sulfur geochemistry of a reactive barrier for treatment of mine drainage. Appl. Geochem. 15, 1331-1343.

Holmström, H., Öhlander, B., 1999. Oxygen penetration and subsequent reactions in flooded sulphidic mine tailings: A study at Stekenjokk, northern Sweden. Appl. Geochem. 14, 747-759.

Holmström, H., Ljungberg, J., Ekström, M., Öhlander, B., 1999. Secondary copper enrichment in tailings at the Laver mine, northern Sweden. Environ. Geol. 38, 327-342.

Hulshof, A.H.M., Blowes, D.W., Ptacek, C.J., Gould, W.D., 2003. Microbial and nutrient investigations into the use of in situ layers for treatment of tailings effluent. Environ. Sci. Technol. 37, 5027-5033.

Hydrological Atlas of Canada, 1978. Fisheries and Environment Canada. Surveys and Mapping Branch, Natural Resour. Can., Ottawa.

Istomina, V.S., 1957. Seepage Stability of Soils. Moscow.

Jacob, D.J., Otte, M.L., 2004. Long-term effects of submergence and wetland vegetation on metals in a 90-year old abandoned Pb-Zn mine tailings pond. Environ. Poll. 130, 337-345.

Jasechko, S., Birks, S.J., Gleeson, T., Wada, Y., Fawcett, P.J., Sharp, Z.D., McDonnell, J.J. Welker, J.M., 2014. The pronounced seasonality of global groundwater recharge. Water Resour. Res., 50, doi:10.1002/2014WR015809.

Kaplan, I.R., Rittenberg, S.C., 1964. Microbiological fractionation of sulphur isotopes. J. Gen. Microbiol. 34, 195– 212.

Knöller, K., Fauville, A., Mayer, B., Strauch, G., Friese, K., Veizer, J., 2004. Sulfur cycling in an acid mining lake and its vicinity Lusatia, Germany. Chem. Geol. 204, 303-323

Kossoff, D., Dubbin, W.E., Alfredsson, M., Edwards, S.J., Macklin, M.G., Hudson-Edwards, K.A., 2014. Mine tailings dams: characteristics, failure, environmental impacts, and remediation. Appl. Geochem. 51, 229-245.

Lewis, B.A. and Gallinger, R.D., 1999. Poirier site reclamation program. In: Proceedings Sudbury'99 Mining and the Environment II, Sudbury, ON, Canada, Vol. 2., pp. 439-448.

Li, M., Aubé, B., St-Arnaud, L., 1997. Consideration in the use of shallow water covers for decommissioning reactive tailings. In: 4th International Conference on Acid Mine Drainage, May 31-June 6, Vancouver, BC, pp. 115-130.

Light, T.S., 1972. Standard solution for redox potential measurements. Anal. Chem. 44, 1038-1039.

Lindsay, M.B.J., Wakeman, K.D., Rowe, O.F., Grail, B.M., Ptacek, C.J., Blowes, D.W., Johnson, D.B., 2011. Microbiology and geochemistry of mine tailings amended with organic carbon for passive treatment of pore-water. Geomicrobiol. J. 28, 229-241.

Lindsay, M.B.J., Condon, P.D., Jambor, J.L., Lear, K.G., Blowes, D.W., Ptacek, C.J., 2009a. Mineralogical, geochemical, and microbial investigation of a sulfide-rich tailings deposit characterized by neutral drainage. Appl. Geochem. 24, 2212-2221.

Lindsay, M.B.J., Blowes, D.W., Condon, P.D., Ptacek, C.J., 2009b. Managing pore-water quality in mine tailings by inducing microbial sulfate reduction. Environ. Sci. Technol. 43, 7086-7091.

Lu, J., Alakangas, L., Jia, Y., Gotthardsson, J., Evaluation of the application of dry covers over carbonate-rich sulphide tailings. J. Hazard. Mater. 244-245, 180-194.

McDonald, C.M., Gould, W.D., Lindsay, M.B.J., Blowes, D.W., Ptacek, C.J., Condon, P.D., 2013. Assessing cellulolysis in passive treatment systems for mine drainage: A modified enzyme assay. J. Environ. Qual. 42, 48-55.

Mineral Resources Branch, 1978. Sherridon Mine. Reference-Manitoba Card #839. A Compendium. Natural Resour. Can., Ottawa.

Moncur, M.C., Ptacek, C.J., Blowes, D.W., Jambor, J.L., 2005. Release, transport and attenuation of metals from an old tailings impoundment. Appl. Geochem. 20, 639-659.

Moncur, M.C., Ptacek, C.J., Blowes, and Jambor, J.L. 2006. Spatial variations in water composition at a Northern Canadian lake impacted by mine-drainage. Appl. Geochem. 21, 1799-1817.

Moncur, M.C., Ptacek, C.J., Mayer, B., Blowes, D.W., Birks, S.J. 2009a. Tracing the sulfur cycle at an abandoned high-sulfide tailings impoundment using chemical and isotopic techniques. In: A. Mehrotra, G. Hao (Eds.) 11th International Symposium on Environmental Issues and Waste Management in Energy and Mineral Production. Banff, AB. November 16-19, pp. 316-324.

Moncur, M.C., Jambor, J.L., Ptacek, C.J., Blowes, D.W., 2009b. Mine drainage from the weathering of sulfide minerals and magnetite. Appl. Geochem. 24, 2362-2373.

Moncur, M.C., Blowes, D.W., Ptacek, C.J., 2013. Pore-water extraction from the unsaturated zone. Can. J. Earth Sci. 50, 1051-1058.

Moncur, M.C., Ptacek, C.J., Hayashi, M., Blowes, D.W., Birks, S.J., 2014. Seasonal cycling and mass-loading of dissolved metals and sulfate discharging from an abandoned mine site in northern Canada. Appl. Geochem. 41, 176-188.

Nelson, S.T., 2000. A simple, practical methodology for routine VSMOW/SLAP normalization of water samples analyzed by continuous flow methods. Rapid Commun. Mass Spectrom. 14, 1044-1046.

Nicholson, R.V., Gillham, R.W., Cherry, J.A., Reardon, E.J., 1989. Reduction of acid generation in mine tailings through the use of moisture-retaining cover layers as oxygen barriers. Canadian Geotech. J 26, 1 -8.

Nordstrom, D.K., 1977. Thermochemical redox equilibria in Zobell's solution. Geochim. Cosmochim. Acta 41, 1835-1841.

Nordstrom, D.K., Alpers, C.N., 1999. Negative pH, efflorescent mineralogy, and consequences for environmental restoration at the Iron Mountain Superfund site, California. Proc. Natl. Acad. Sci. 96, 3455-3462.

Ouangrawa, M., Molson, J., Aubertin, M., Bussiere, B., Zagury, G.J., 2009. Reactive transport modeling of mine tailings columns with capillary-induced high water saturation for preventing sulfide oxidation. Appl. Geochem. 24, 1312-1323.

Paktunc, A.D., Davé, N.K., 2002. Formation of secondary pyrite and carbonate minerals in the Lower Williams Lake tailings basin, Elliot Lake, Ontario, Canada. Amer. Mineral. 87, 593–602.

Papelis, C., Hayes, K.F., Leckie, J.O., 1988. HYDRAQL: A program for the computation of chemical equilibrium composition of aqueous batch systems including surface complexation modeling of ion adsorption at the oxide/solution interface. Technical Report 306, Stanford University, Palo Alto, California.

Pedersen, T.F., 1985. Early diagenesis of copper and molybdenum in mine tailings and natural sediments in Rupert and Holberg inlets, British Columbia. Can. J. Earth Sci. 22, 1474-1484.

Pedersen, T.F., Mueller, B., McNee, J.J., Pelletier, C.A., 1993. The early diagenesis of submerged sulphide-rich mine tailings in Anderson Lake, Manitoba. Can. J. Earth Sci. 30, 1099-1109.

Poling, G.W., Ellis, D.V., Murray, J.W., Parsons, T.R., Pelletier, C.A., 2002. Underwater tailings placement at Island Copper Mine: A success story. Soc. Mining, Metallurgy and Exploration, Inc. Littleton, CO, pp.204

Ptacek C.J., Blowes, D.W., 1994. Influence of siderite on the pore-water chemistry of inactive mine-tailings impoundments. Environmental Geochemistry of Sulfide Oxidation. (C.N. Alpers and D.W. Blowes, eds.), American Chemical Society, Symposium Series Vol. 550, pp. 172-189.

Rasmuson, A., Collin, M., 1988. Mathematical modelling of water and oxygen transport in layered soil covers for deposits of pyritic mine tailings. In: Proceedings Internat. Conf. Control Environ. Problems from Metal Mines, Roros, Norway, pp. 32.

Ravel, B., Newville, M., 2005. ATHENA, ARTEMIS, HEPHAESTUS: data analysis for X-ray adsorption spectroscopy using IFEFFIT. J. Synchrotron Radiat. 12, 537–541.

Reardon, E.J. and Moddle, P.M., 1985. Gas diffusion measurements on uranium mill tailings: implications to cover layer design. Uranium 2, 111-131.

Robertson, J.D., 1992. Subaqueous disposal: a promising method for the effective control of reactive waste materials. In: 24th Annual Meeting of the Canadian Mineral Processors Conference, January 21-23, Ottawa, ON, Paper 33. p. 10.

Robertson, W.D., 1994. The physical hydrogeology of mill-tailings impoundments. In: Jambor, J.L., Blowes, D.W. (Eds.), Environmental Geochemistry of Sulfide Mine-Wastes. Mineral. Assoc. Can. Short Course Vol. 22, 271-292.

Robertson, J.D., Tremblay, G.A., Fraser, W.W., 1997. Subaqueous tailings disposal: A sound solution for reactive tailings. In: 4th International Conference on Acid Rock Drainage, May 31-June 6, Vancouver, BC, Canada, Vol. 3, pp. 1027-1044.

Rowe, R.K., Hosney, M.S., 2013. Laboratory investigation of GCL performance for covering arsenic contaminated mine wastes. Geotext. Geomembr. 39, 63-77.

Rye, R.O., Bethke, P.M., Wasserman, M.D., 1992. The stable isotope geochemistry of acid sulfate alteration. Econ. Geol. 87, 225–262.

Samad, M.A., Yanful, E.K., 2005. A design approach for selecting the optimum water cover depth for subaqueous disposal of sulfide mine tailings. Can. Geotech. J. 42, 207-228.

Seal, R.R., 2003. Stable-isotope geochemistry of mine waters and related solids. In: Jambor, J.L., Blowes, D.W, Ritchie, A.I.M. (Eds.), Environmental Aspects of Mine Wastes. Mineral. Assoc. Can. Short Course Vol. 31, pp. 303-334.

SMEWW (Standard Methods for the Examination of Water and Wastewater), 2005. American Health Association, Washington, D.C.

Sodermark, B., Lundgren, T., 1988. The Bersbo project - The first full scale attempt to control acid mine drainage in Sweden. In: Proceedings Internat. Conf. Control Environ. Problems from Metal Mines, Roros, Norway, p. 17.

Tassé, N., Germain, M.D., Bergeron, M., 1994. Composition of interstitial gases in wood chips deposited on reactive mine tailings. In: Alpers, C.N., Blowes, D.W. (Eds.), Environmental geochemistry of sulfide oxidation. Am. Chem. Soc. Symp. Series, 550, 631-634.

Taylor, B.E., Wheeler, M.C., Nordstrom, D.K., 1984. Stable isotope geochemistry of acid mine drainage: Experimental oxidation of pyrite. Geochim. Cosmochim. Acta 48, 2669-2678.

Tuttle, J.H., Dugan, P.R., Randles, C.I., 1969. Microbial sulfate reduction and its potential utility as an acid mine water pollution abatement procedure. Appl. Microbiol. 17, 297-302.

Vigneault, B., Campbell, P.G., Tessier, A., De Vitre, R., 2001. Geochemical changes in sulfidic mine tailings stored under a shallow water cover. Water Res. 35, 1066-1076.

Vigneault, B., Kwong, Y.T.J., Warren, L., 2007. Assessing the long term performance of a shallow water cover to limit oxidation of reactive tailings at Louvicourt Mine. MEND Report 2.12.2.

Yanful, E.K., Aube, B.C., Woyshner, M., ST-Arnaud, L.C., 1994. Field and laboratory performance of engineered covers on the Waite Amulet tailings. In: Internat. Land Reclamation Mine Drainage Conf. and Third Internat. Conf. Abatement Acidic Drainage Vol. pp. 8-147, U.S. Dept. Interior, Bureau of Mines Special Publication SP 06A-94.

Yanful, E.K., Simms, P.H., 1997. Review of Water Cover Sites and Research Projects, p. 136. MEND report 2.18.1.